Engineering Structures 298 (2024) 117068

Contents lists available at ScienceDirect

Engineering Structures

journal homepage: www.elsevier.com/locate/engstruct

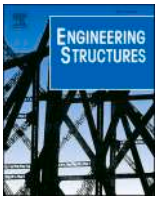

Structural performance study and improvement of Artemio Franchi Stadium in Florence

Gloria Terenzi [a,*], Elena Fuso [b], Stefano Sorace [b]

[a] Department of Civil and Environmental Engineering, University of Florence, Via S. Marta 3, 50139 Florence, Italy
[b] Polytechnic Department of Engineering and Architecture, University of Udine, Via delle Scienze 206, 33100 Udine, Italy

ARTICLE INFO

Keywords:
Heritage reinforced concrete structures
Diagnostic investigation
Static assessment
Seismic assessment
Seismic retrofit
Dissipative braces
Fluid viscous dampers

ABSTRACT

Artemio Franchi Stadium in Florence is the first world-famous work by Pier Luigi Nervi, and is celebrated as a masterpiece of the Rationalist movement. In view of this, it has been declared a work of cultural and historical interest by the Italian Ministry for Cultural Heritage and Activities, with several specific preservation restrictions on its most distinguishing structural and architectural elements. With a view to the recently planned restyling and modernization works, a diagnostic field survey and testing campaign, and a static and seismic performance assessment study of the Stadium were commissioned by the Municipality of Florence. Furthermore, a retrofit design respectful of the architectural preservation requirements was requested for its reinforced concrete structure. The contents of the diagnostic and assessment study, as well as of the retrofit design, are presented in this paper. The results of the structural analyses, carried out by means of a detailed finite element model calibrated on the field survey and testing data, show slightly unsafe static conditions in less than 10% of the beams and columns constituting the bleacher sloped frames, and diffused unsafe conditions under seismic action scaled at the Basic Design Earthquake level. The proposed retrofit solution consists in incorporating dissipative braces equipped with fluid viscous spring-dampers in several spans oriented in orthogonal direction to the bleacher frames, and installing fluid viscous pure dampers across the majority of the technical separation gaps between adjacent bleacher blocks, so as to prevent their mutual pounding. The results of the analyses in retrofitted conditions highlight a transition to safe conditions for more than half of the unsafe members, and a remarkable reduction of the demand/capacity ratios in the remaining members. Safe stress states can be reached in the latter by means of simple additional local strengthening interventions. This substantial improvement of seismic performance is achieved with a minimal visual and functional impact on the existing structures, as prescribed by the imposed preservation restrictions.

1. Introduction

The “art of modern structural engineering” [1–2] marks its main achievements with iron and steel structural works until the last decade of the 19th century. Subsequently, the growing use of reinforced concrete (RC), in parallel with the evolution in steel construction, allows overcoming new challenges in terms of structural shapes, cosmetic value, efficiency, functions, heights, spans, costs, and use of sources and resources. This season sees Hennebique, Freyssinet and Maillart among the main innovators, to whom new generations of recognized structural designers follow in the first three decades of the 20th century. Within these new generations, a leading figure is Pier Luigi Nervi, whose design philosophy, which admirably joins art, science and functionality [3–4], finds correspondence in the works of his contemporary (Eduardo Torroja, Ove Arup, Giorgio Morandi, etc.) and following (Felix Candela, Fazlur Kahn, Sergio Musmeci, Christian Menn, etc.) structural engineer “artists” [5–6].

The first world-famous Nervi’s design is Artemio Franchi Stadium in Florence, formerly named “Giovanni Berta” and then “Comunale” (Municipal) Stadium, celebrated as a masterpiece of the Rationalist movement since its construction, carried out in 1930–1932 [7–12]. This acknowledgment derives from the innovative D-shaped plan and “telescope”-like appearance of the bleachers ring in perspective, and the neat exposed structure, constituted by elegant rhythmically repeated RC sloped frames. These features are highlighted by the photographic images in Fig. 1, showing the final architectural model of the Stadium and

* Corresponding author.
E-mail address: gloria.terenzi@unifi.it (G. Terenzi).

https://doi.org/10.1016/j.engstruct.2023.117068
Received 2 July 2023; Received in revised form 29 September 2023; Accepted 17 October 2023
Available online 24 October 2023
0141-0296/© 2023 The Authors. Published by Elsevier Ltd. This is an open access article under the CC BY-NC-ND license (http://creativecommons.org/licenses/by-nc-nd/4.0/).

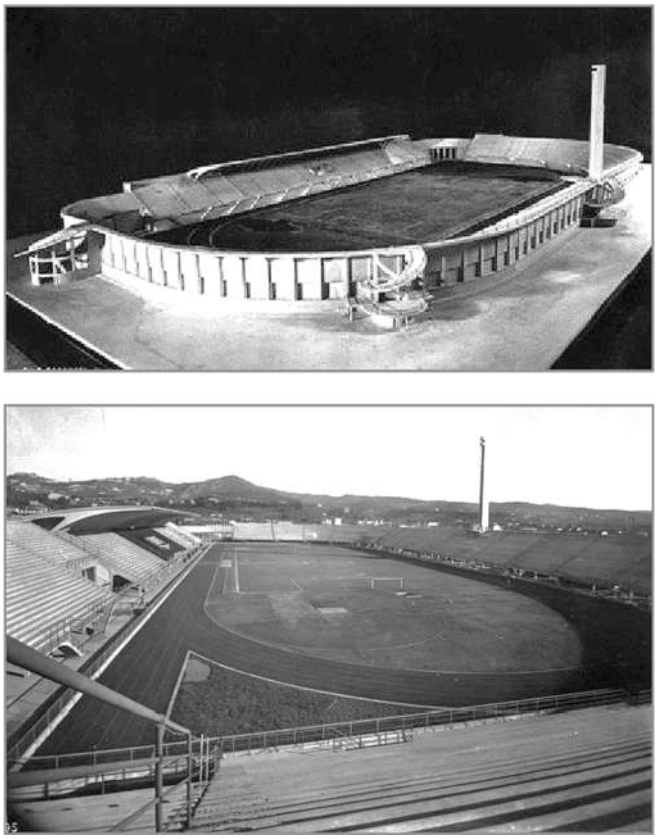

Fig. 1. Final architectural model of the Stadium, and internal view in 1932 (photographic archive Barsotti, Florence).

an internal view of it taken in 1932, soon after the completion of the bleacher ring, and in Fig. 2, displaying external views of the same year. Other prominent and distinguishing elements are represented by the Tribuna Centrale (main stand) cantilevered roof—exhibiting the widest RC free span worldwide at the time of construction and for the following twenty years, equal to 22.5 m—, the bold and aerial helical staircases giving access to Curva Fiesole, Curva Ferrovia stands and Maratona grandstand, the slender iconic Maratona Tower, and the elliptical balcony scenically jutting out of the elevation portion of the latter from on top of the Maratona bleachers. Images of these structures taken during the construction works and immediately after their completion are shown in Figs. 3 through 5. Fig. 3 highlights the rhomboidal steel reinforcing mesh of the helical staircases slab, representing a reinforcement solution typically adopted by Nervi in all RC slabs of the Stadium, as well as in other structures belonging to the same period; reinforcement details of the helical beam bearing the slab and the crossed helical beam providing support to the latter in correspondence with its center section; and the completed staircases. Fig. 4 illustrates the complex scaffolding system used for the construction of the cantilevered roof of Tribuna Centrale main stand, the original drawing of its structural section and the upper portion of the supporting sloped frames, and an image of the loading configuration of two transversal spans adopted for the final tests on the roof, made of sand and gravel bags. The construction of Maratona Tower balcony, showing the reinforcement of the constituting cantilever rib beams, annular edge beam and rhomboidal steel mesh, and images of the Tower during and at the end of construction, are illustrated in Fig. 5.

Based on its architectural and engineering prominence, the Stadium has been declared an artefact of cultural and historical interest pursuant to Legislative Decree No. 42 of 22 January 2004 (Code of Cultural and Landscape Heritage) [13] by the Ministry for Cultural Heritage and Activities (currently named Italian Ministry of Culture). As a consequence, it has been subjected to general protection constraints on its whole RC structure, and specific strict constraints on the above-mentioned most valued building portions (Tribuna Centrale roof,

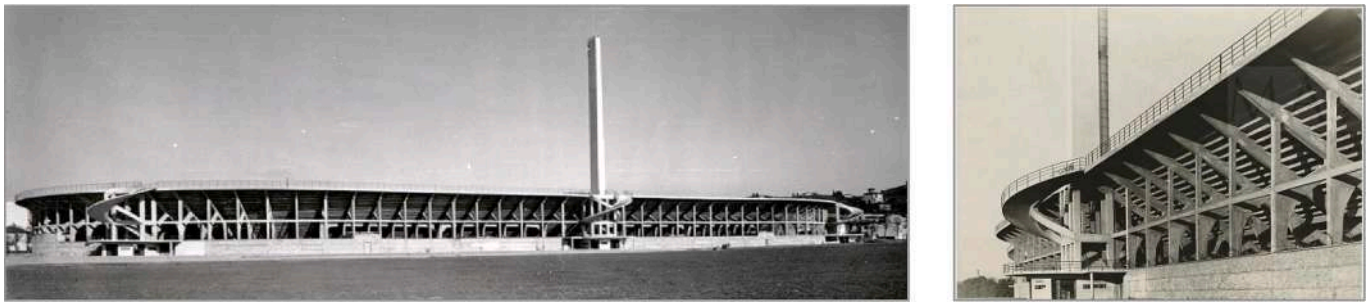

Fig. 2. External views of the Stadium in 1932 (photographic archive Barsotti, Florence).

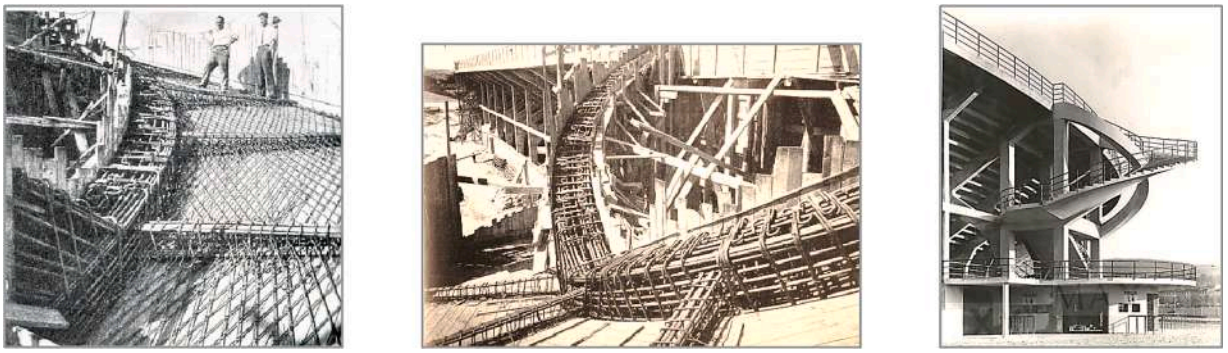

Fig. 3. Views of the reinforcement of slabs and beams of the helical staircases, and their appearance at the end of the construction works (photographic archives Barsotti, Florence – left and right image, and of the Municipality of Florence – central image).

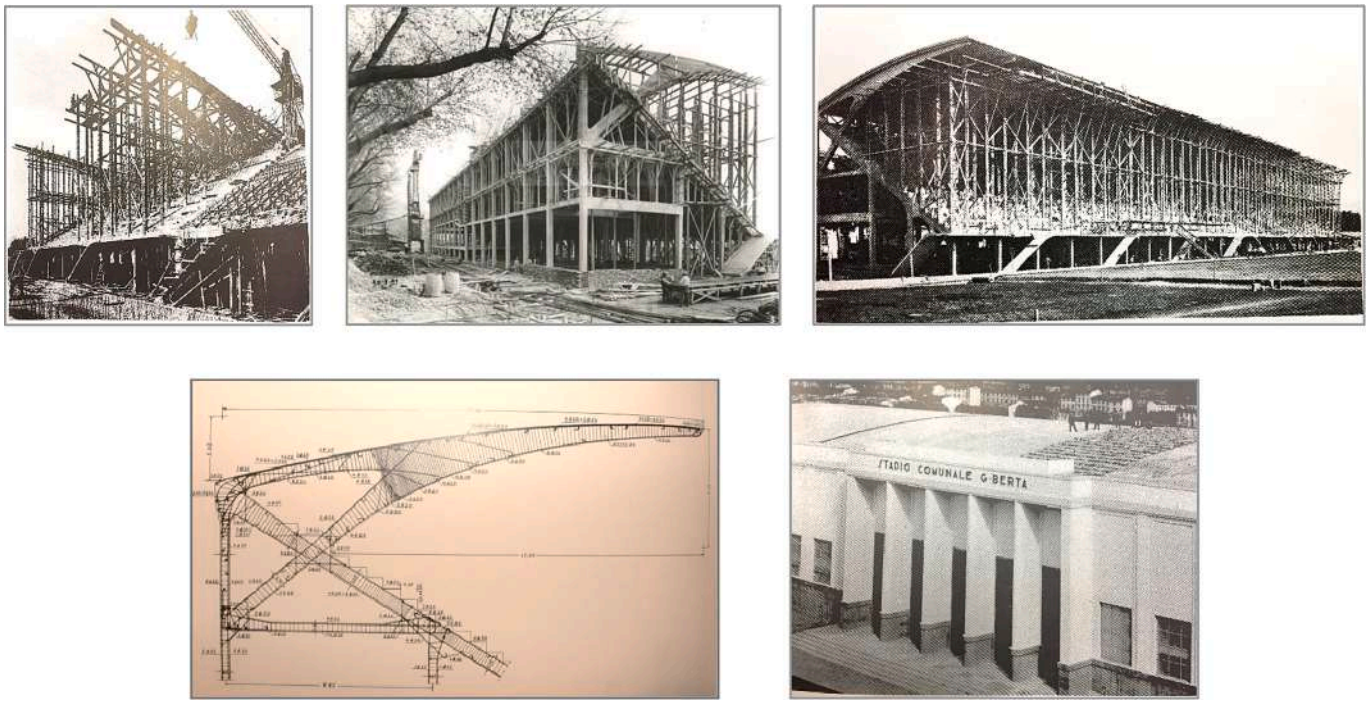

Fig. 4. Views of the scaffolding system of the cantilevered roof of Tribuna Centrale stand, original design drawing of its structural section and the upper portion of the supporting sloped frames, and loading configuration adopted for the final tests on roof portions (photographic archives Barsotti, Florence – top images, and of the Municipality of Florence – bottom images).

Fig. 5. Views of the reinforcement of Maratona Tower balcony (photographic archive Locchi, Florence), and images of the Tower during (idem) and at the end of construction works (photographic archive Barsotti, Florence).

helical staircases, Maratona Tower).

At the same time, the Ministry of Culture recently financed—with the economic support of the European Community—a thorough architectural and functional refurbishment intervention of the Stadium, aimed at making it compliant with the current highest UEFA standards, based on the winning project of an international design competition. According to the imposed protection constraints, this project entirely preserves the original structure, while at the same time adding new structurally independent stands and a new roof—structurally independent too—over the uncovered stands.

With a view to the development of this competition, the Municipality of Florence commissioned a static and seismic assessment study of the structure of the Stadium, as well as a retrofit design aimed at guaranteeing its safe use in current conditions and after the planned architectural refurbishment interventions. The structural analysis was based on a careful recognition of the original design documentation, and extensive field surveys and on-site diagnostic testing campaigns, according with the approaches recently adopted in the evaluation of older RC buildings of architectural value [14–18]. The proposed retrofit solution consists in incorporating dissipative braces equipped with fluid viscous spring-dampers in several spans oriented in orthogonal direction to the bleachers bearing frames, and installing fluid viscous pure dampers across most technical separation gaps between adjacent bleacher blocks.

An overview of the assessment and retrofit design study is offered in

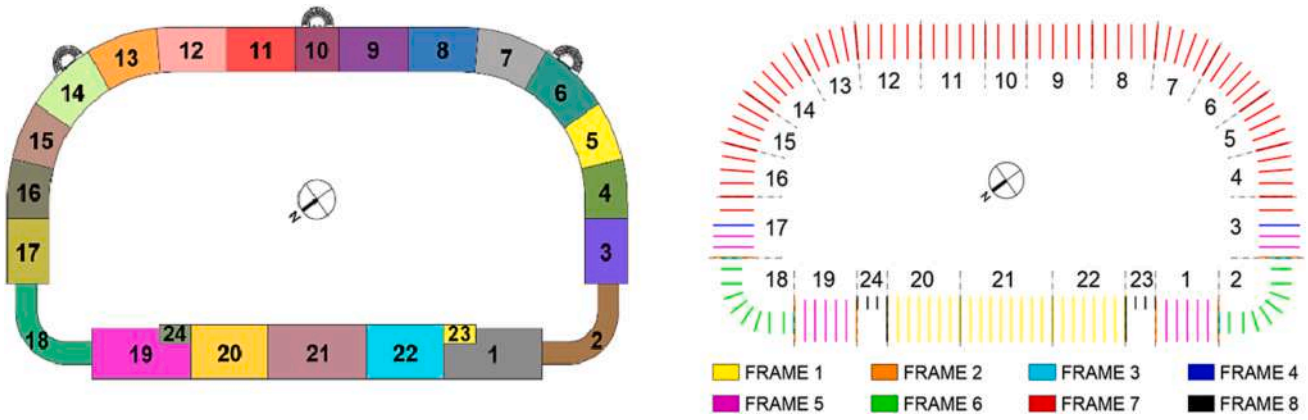

Fig. 6. Blocks and RC frame types constituting the Stadium in plan.

this article. The general architectural and structural characteristics of the Stadium, and selected results of the experimental campaigns on the structural materials and members, as well as of the dynamic tests developed on some bleacher blocks and Maratona Tower, are initially described. The finite element model generated for the whole structure, calibrated on the data collected through the diagnostic investigations, and the results of the static and seismic assessment analyses carried out by this model, are then presented. Details of the retrofit intervention are also illustrated, and the results of the analyses in rehabilitated conditions are discussed. The latter highlight a substantial improvement of seismic performance as compared to the current state, with minimal visual perception on the existing structures, and no impact on the redevelopment and modernization works planned for the Stadium, as targeted in this design.

2. Architectural and structural characteristics of the Stadium

The structure of the Stadium consists of 24 blocks separated by technical gaps (Fig. 6a), constituted by eight different types of RC sloped frames (Fig. 6b). The cross sections of the latter are represented in the graphics of Fig. 7, redrawn from the original design documentation. An annular beam, constituting the first step of all frame types, except for type 6 frames, connects blocks 3 through 17, and 1 through 19 (passing from blocks 20 through 23). An aerial view of the Stadium in its current state is displayed in Fig. 8, showing the additions made during the refurbishment works carried out for the World Football Championship of 1990 (the most important of which are the Curva Fiesole and Curva Ferrovia RC parterre bleachers, the completion of the bleachers under the "connection" blocks 2 and 18 with a steel structure, and the steel cantilever roofs covering the two Tribuna Centrale lateral blocks).

From a structural viewpoint, the most complex block is number 10, which incorporates Maratona Tower and the helical staircases of relevant grandstand. The Tower has a total height of 53.68 m above the ground, and is constituted by a 39.43 m-high RC core structure standing out from four columns on top of the bleachers, situated at 13.65 m above the ground (Fig. 9). The four columns, sized (700 × 700) mm^2, are mutually connected in longitudinal direction by two Vierendell-type beams. The RC core of the Tower is 500 mm-thick from the base to the first level (ending at 28.15 m), 300 mm-thick up to the second level (41.18 m) and 100 mm-thick up to the top. The internal section of the core has a constant size of 1.65 m × 1.15 m and hosts an elevator. The Tower is completed on the field side by a semi-elliptical glass surface borne by a steel frame structure, and ends with a flagpole, the top of which reaches a height of 71 m above the ground. The helical staircases, located on the rear of the Tower, are 2.4 m wide, have a radium of 6.66 m and connect the top of the two underlying straight flights of stairs, situated at a height of 7.15 m, to the top of the grandstand. Width and radium are the same as for the helical staircases of Curva Fiesole and Curva Ferrovia stands. The foundations of all columns are constituted by parallelepiped RC footings built over a lean concrete layer.

3. On-site experimental campaign

3.1. Tests on materials and structural members

This section of the investigation campaign included: 127 pacometer tests (denoted with abbreviation "PAC" in the sketches of Fig. 10) and 11 geo-radar tests for non-invasive checks on steel reinforcement; 137 concrete cover demolitions with geometrical checks of the underlying reinforcing bar diameters ("S"); 60 SonReb tests (i.e. combined sclerometer—"SON"—and ultrasonic tests—" SO"); 22 core drillings ("C") with on-site carbonation tests, and compression strength laboratory tests on the cylindrical concrete samples; 3 extractions of reinforcing bars, with tension strength laboratory tests; and 13 on-site Vickers durometer tests on exposed bars, to estimate hardness and strength of the constituting steel. Fig. 10 particularly shows: concrete samples drilled from columns belonging to one type 7 frame of block 9 (Fig. 10a) and one type 1 frame of block 21 (Fig. 10b), with the pigmentation resulting from the carbonation tests carried out with phenolphthalein alcoholic solution spray (highlighting that the carbonation depth is at most limited to the concrete cover thickness); concrete cover demolitions following a series of pacometer tests, with measurement of the exposed bar diameters, on columns belonging to one type 7 frame of block 5 (Fig. 10c) and block 10 (Fig. 10d); and georadar surveys carried out on one type 7 frame of block 11 (Fig. 10e,f).

Consistently with the prescriptions of the Italian Technical Standards [19] and relevant Commentary [20], the compression strength was evaluated as weighted average value, f_{cm}, of the results of the laboratory tests on the extracted samples and the on-site SonReb tests. The following f_{cm} values were derived: 24.76 N/mm^2, for members belonging to Curva Ferrovia blocks; 28.03 N/mm^2 (Maratona); 25.19 N/mm^2 (Curva Fiesole); 25.47 N/mm^2 (Tribuna Centrale); 30.04 N/mm^2 (helical staircases); and 46.17 N/mm^2 (Maratona Tower). These values highlight a comparable quality of concrete adopted for the various stands, and a higher quality for Maratona Tower, as also attested by the acceptance test reports of the time. The average yield stress of the steel constituting the three extracted bars obtained from the laboratory tests is equal to f_{ym} = 316.3 N/mm^2. The durometer tests substantially confirmed this value. Moreover, a satisfactory conservation state was observed, 90 years after the construction of the RC structures, for all the bars exposed by cover demolition, with oxidation never exceeding a physiological surface level.

3.2. Dynamic tests on the structure

The dynamic characterization tests were carried out with a special

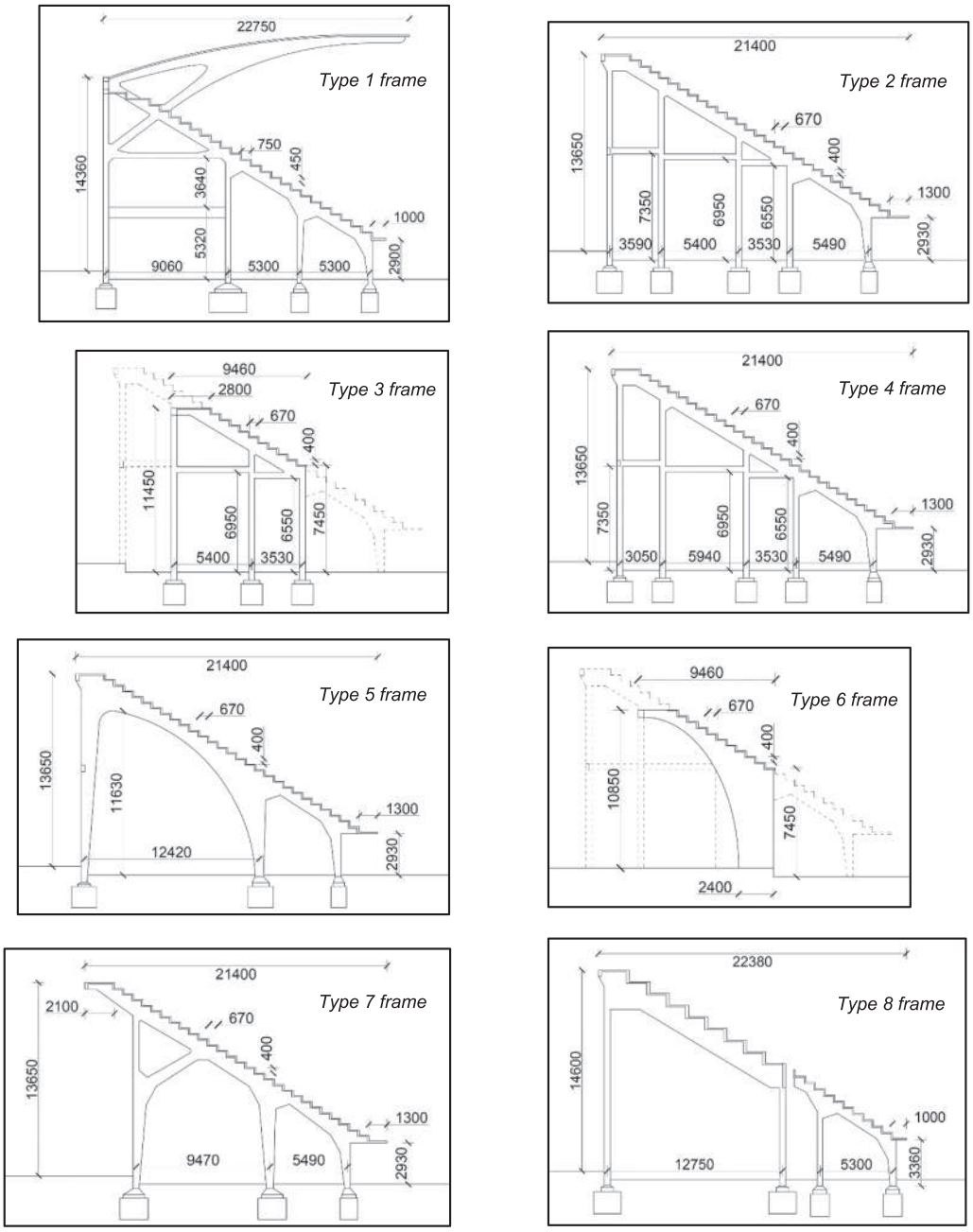

Fig. 7. Geometry of the eight types of frames (dimensions in millimeters).

radar interferometric technique [21], based on the use of a portable radar sensor equipment transmitting continuous waves at discrete frequency values, with 16.75 GHz center frequency and up to 350 MHz bandwidth. The sampling frequency is tuned on the exciting action, and for rather high or wide structures it normally ranges from 50 Hz to 100 Hz. The equipment includes two horn transmitting and receiving antennas with half power band width of about 13°. The radiated electromagnetic waves are reflected by the structures and captured by an internal receiver, providing displacement measurements with sub-millimetric resolution.

The acquired displacement time-histories are elaborated via Joint Time Frequency Analysis (JTFA), which evaluates the Fourier transform of the displacement signals by a sliding time-window. The main natural vibration frequencies of the investigated structure are estimated by averaging the amplitudes of the spectra obtained for several consecutive time windows, yielding more accurate results as compared to a Fourier Transform Analysis performed on the complete displacement time-histories. The portable radar can be freely installed in various different positions on—or above—ground, and can perform measurements for different targets of the structure, optionally installing special reflectors on it.

The interferometric technique was applied to identify the main vibration frequencies of Maratona Tower and some stand blocks, using wind and the loads induced by the public in the bleachers as input actions. An image of the radar equipment installed in the football playing field for a survey carried out on the Tower under wind action is shown in Fig. 11. The average wind peak velocities measured during these tests were equal to about 10 m/s. The positions of the radar equipment during two football matches, attended by about 30,000 spectators in both cases, are located with red dots in the schematic plans of Fig. 12. As highlighted by these drawings, the investigated blocks were: 9, 11, 14, 18 and 19, during the first match, and again 9, 11, 14 (to perform a

Fig. 8. Current aerial view of the Stadium.

comparison with the results of the first survey), plus 3 and 5, during the second match. Practically coinciding values of the three main vibration frequencies were deduced for the Tower from the wind and spectators-induced responses, that is: $f_{1,MT} = 0{,}685$ Hz (rotational mode around the vertical axis), $f_{2,MT} = 0{,}799$ Hz (translational mode in transversal direction, parallel to the X local reference axis shown in the drawing of Fig. 13), and $f_{3,MT} = 1{,}031$ Hz (translational mode in longitudinal direction, parallel to the Y axis). By way of example of the results obtained for the blocks, the following first two frequencies were identified for number 14: $f_{1,B14} = 2.83$ Hz, and $f_{2,B14} = 5.04$ Hz, related to the first translational modes in orthogonal and parallel direction to the constituting frames.

It can be observed that, while the portable radar sensor is a very simple device as compared to sensor nets wired to central recording systems, it has always given accurate results in dynamic characterization campaigns of large structures and infrastructures [21]. The installation of an extended sensor net, not financed at this stage, was planned to serve as permanent monitoring system after the upcoming architectural and functional refurbishment intervention of the Stadium will be completed.

A check on the results of the radar survey for Maratona Tower was carried out by means of an accelerometer placed on its roof terrace (photographic image in Fig. 13), in similar wind conditions, i.e. with average peak velocities of about 11 m/s. The device was oriented along three different directions, i.e. parallel to the axis of the radar survey performed with the sensor placed in the football field, for a direct comparison with this measurement direction, parallel to X, and parallel to Y. The results highlight frequency values close to the ones identified by the radar campaign, that is, $f_{1,MT} = 0.677$ Hz, $f_{2,MT} = 0.787$ Hz, and $f_{3,MT} = 1.013$ Hz.

4. Finite element model of the Stadium

The finite element analyses of the structure were carried out by means of SAP2000NL software [22]. At a first step, simplified models of the eight sloped frame types were generated, where the sloping beams were simulated by means of uniaxial frame-type elements. These models were then assembled in the 24 blocks. Subsequently, more refined modelling criteria were adopted, and the updated blocks were combined in one final model of the whole structure. By way of example of the criteria followed in the generation of the refined models, Fig. 14 shows the mesh adopted for type 1 sloped frames, and a detail of the connection of the beam with the first column on the field side. As highlighted by these plots, the sloped beams, as well as Tribuna Centrale cantilever roof beams, were discretized by means of shell elements. The latter were finally adopted in consideration of the massive sections of these members, and to geometrically reproduce in detail the saw-tooth shape designed to bear the L-joists constituting the bleachers, for the sloped beams, and the varying curved bifurcated shape, for the roof beams. Section cuts were used to deduce the stress states in beams from the ones computed in the shell elements. The geometrical compatibility conditions between sloped beams and columns were imposed in the joints highlighted by red dots in Fig. 14. The results obtained with these refined models were compared to the ones from the original simple models, for the sake of proper checking. Output stress states were well related in general; as expected, more accurate and detailed data in the most critical sections of the sloped beams and cantilever roof beams have come from the most refined meshes.

The heavy infills of the Tribuna Centrale blocks, originally built in contact with the adjacent RC members, were also modelled by means of shell elements matching their geometry. Equivalent non-linear strut-type [23–24] or other models were not adopted in these analyses, since the incorporation of the panels is essentially aimed at measuring their stiffening effects on the dynamic response of the relevant blocks.

On the other hand, the massive RC footings of columns were not included in the finite element model of the structure, as they were assumed as equivalent fixed-end constraints at the column base sections. The maximum stress states computed in these sections were transferred at the footing base sections in separate calculations, which helped carry out the necessary checks on the underlying foundation soil. All these checks were successful, as a consequence of the adequate dimensions of the footings and the rather good soil characteristics (categorized as C-type soil according to the Italian Technical Standards, as mentioned in

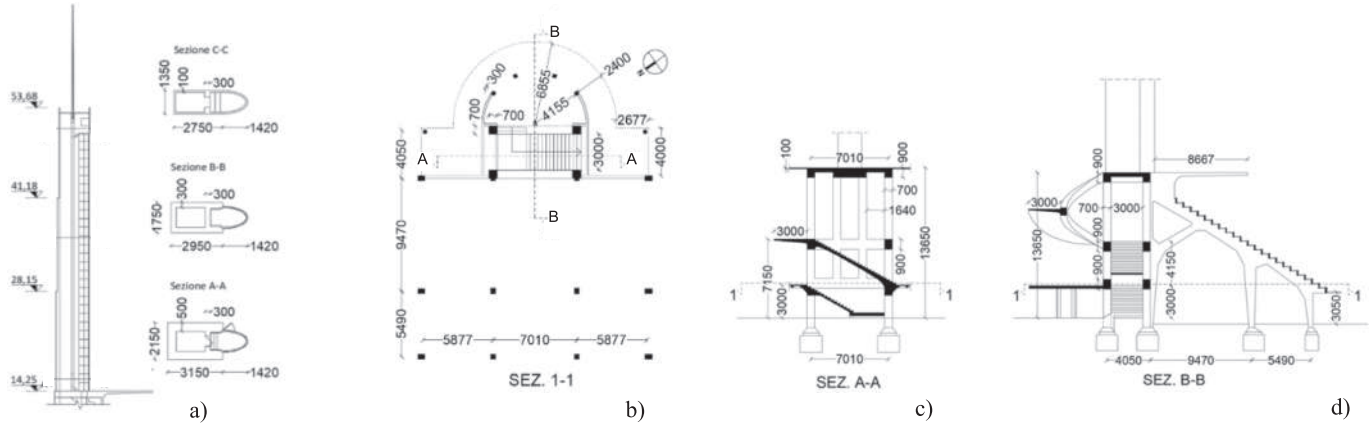

Fig. 9. Lateral view and cross sections of Maratona Tower (a, b), and vertical sections of block 10 at the base of the Tower (c, d) – dimensions in meters (Tower elevation) and millimeters (sections).

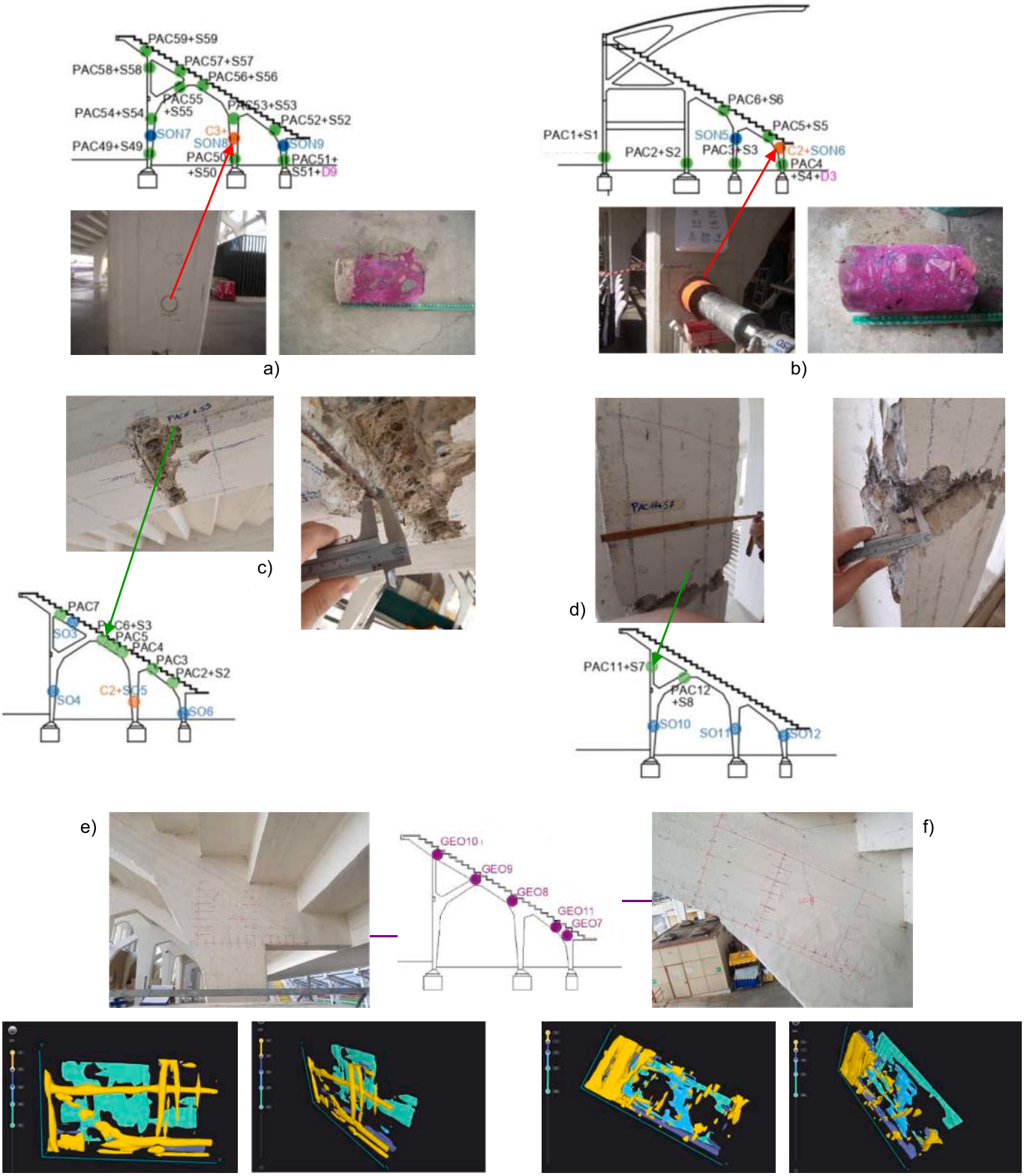

Fig. 10. Images of concrete samples extracted by core drilling, after carbonation tests (a-b), measurement of diameters of bars exposed by cover demolition (c-d), with locations in relevant frames, and georadar surveys (e-f).

Section 5).

A view of the complete finite element model, also including the above-mentioned steel additions built within the restyling interventions carried out in 1989–90 (cantilever roof of blocks 1 and 23, and 19 and 24, bottom bleachers of blocks 2 and 18), is displayed in Fig. 15, along with some detail views extracted from it. The model is constituted by 8,747 frame elements and 32,904 shell elements in total. In consideration of such a large number of elements, the analyses in current state were developed in the elastic field, by extracting the maximum stress states deriving from the most severe load combinations for all structural

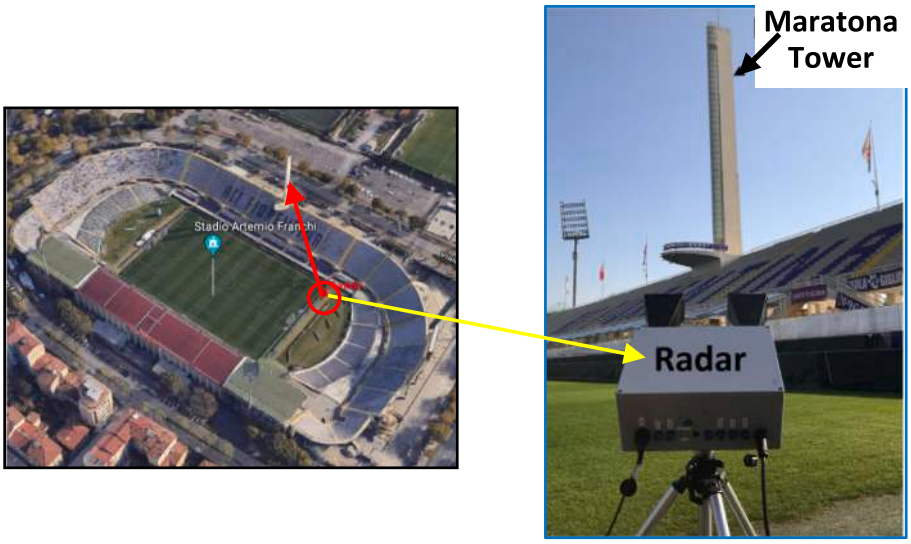

Fig. 11. Positioning of the radar sensor equipment within the playing field for a dynamic survey on Maratona Tower under wind action.

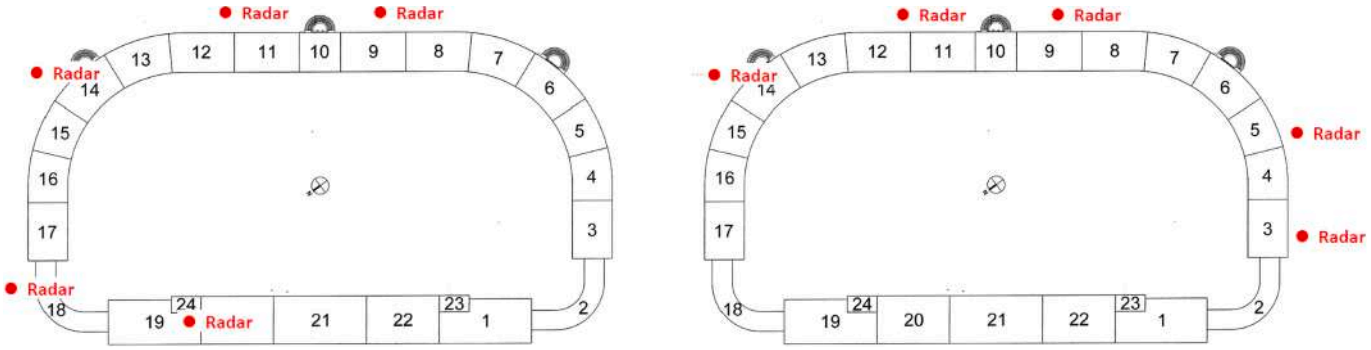

Fig. 12. Positioning of the radar sensor equipment during the first (left) and second (right) football matches.

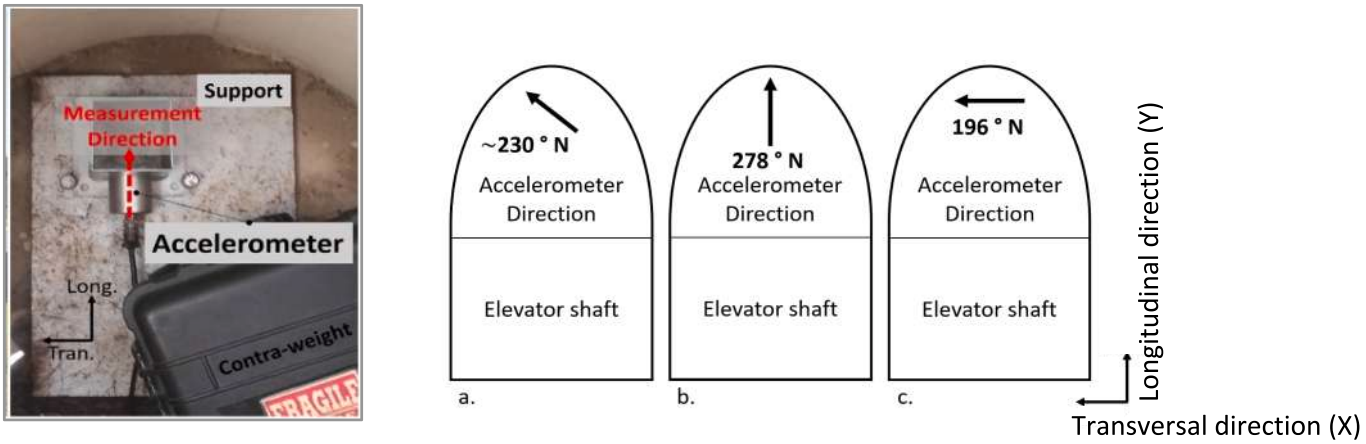

Fig. 13. Accelerometer placed on the roof top of Maratona Tower, and schematic representation of its three installation layouts.

members, and checking them at the ultimate limit states. Potential pounding between adjacent blocks was not simulated, in order to keep the computational burden within acceptable limits too. Indeed, by considering the number of blocks and their possible collision spots, a huge effort would result even if simplified finite element contact models were adopted, like the ones implemented in previous works by the authors [25–26]. Therefore, potential pounding in current conditions was simply checked by comparing the maximum relative displacements of all adjacent blocks with the corresponding mutual separation gap widths. As discussed in Section 6, the effectiveness of the proposed seismic retrofit intervention was evaluated in terms of stress state reductions induced in all structural members, as well as of pounding prevention between all blocks.

The information gained on the mechanical properties of the materials and their current conservation state, as well as on the geometrical and reinforcement details of the structural members, was transferred in

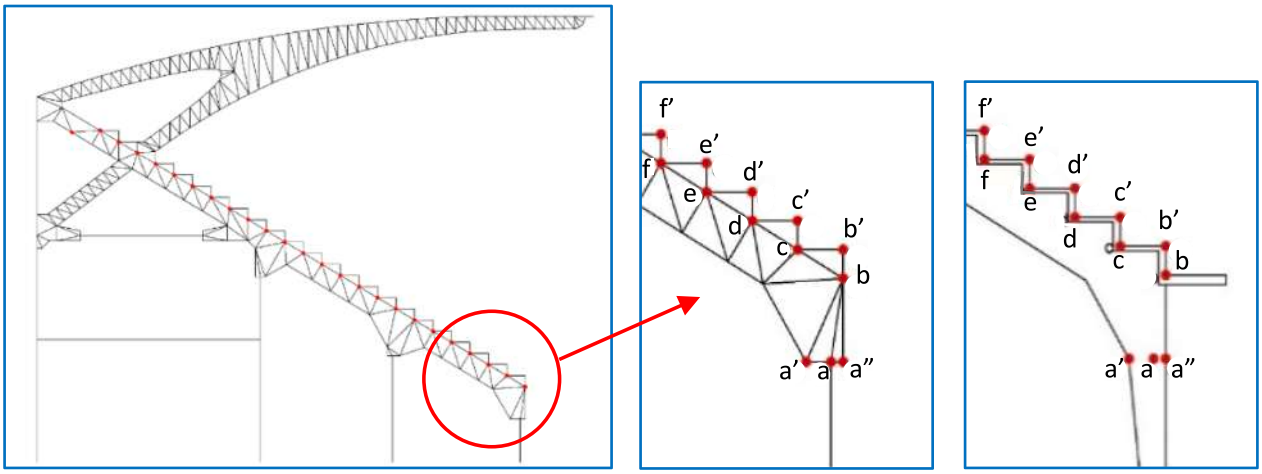

Fig. 14. Finite element model of type 1 frame, and detailed view of the bottom beam-to-column joint and its connection to the bleacher beams.

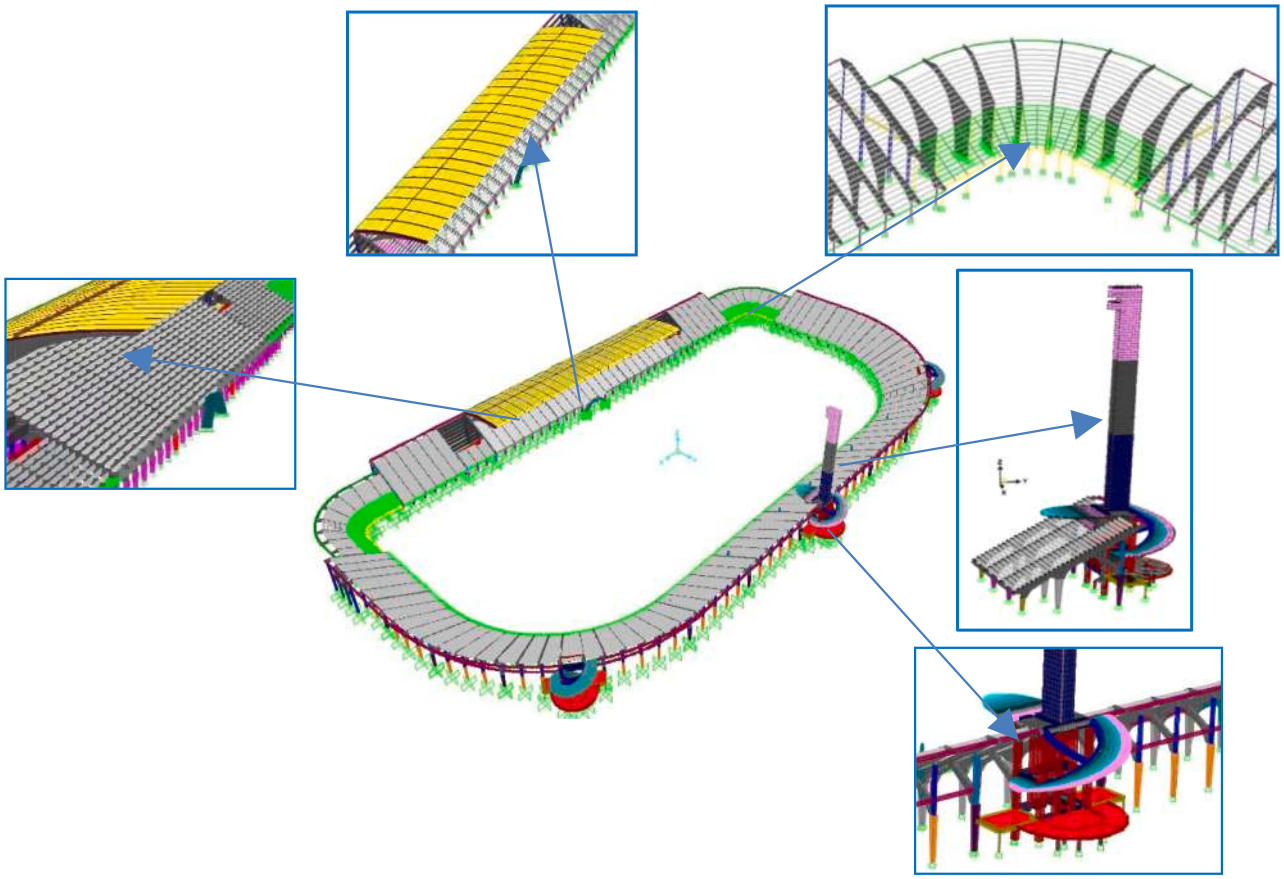

Fig. 15. View of the finite element model of the Stadium, and details of extracted portions.

the computational analyses and the stress state and displacement checks. The experimentally estimated main vibration frequencies helped calibrating further the model, by comparing these values with the results of the modal analyses carried out on the single blocks and Maratona Tower.

The material, static and dynamic structural investigation data allowed also formally reaching the highest "knowledge level" established by the Italian Technical Standards in the assessment of existing buildings. The corresponding value of the "confidence factor", i.e. the additional knowledge level-related safety coefficient to be introduced in the verification checks, was consistently put as equal to 1.

5. Static and seismic assessment analyses

The static analyses carried out at the ultimate limit state by referring to the normative dead and live gravity loads, and relevant combinations, highlight 87 sections in slightly unsafe conditions in flexure and compression-flexure. The demand/capacity ratios, $\alpha_{D/C}$, are no greater than 1.5 for these members, with average values of 1.25 for columns and 1.18 for beams. Shear stress checks are always met, both for the shear-compression and shear-tension mechanisms, as a consequence of the redundant sizes adopted in the original design—developed by referring to the Italian Technical Standards of the time [27]—for the most stressed

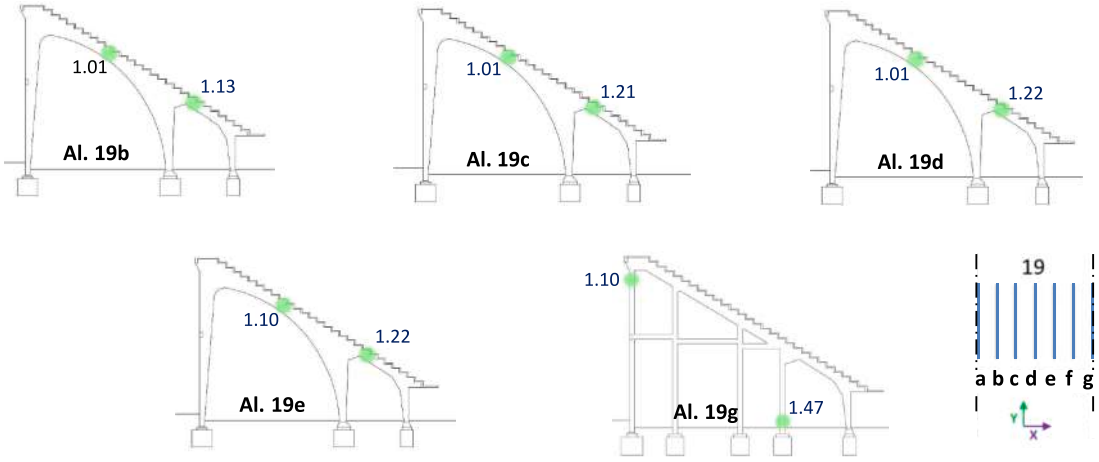

Fig. 16. Static analyses. Sections in unsafe conditions in compression-flexure (highlighted by green dots), and relevant demand/capacity ratios, for the frames belonging to block 19, with associated alignment numbering. (For interpretation of the references to colour in this figure legend, the reader is referred to the web version of this article.)

Fig. 17. Local static strengthening and restoration interventions.

sections, and particularly for the beam-to-column joints. By way of example of the results of static check analyses, Fig. 16 shows the sections in unsafe conditions for the frames belonging to block 19, and relevant $\alpha_{D/C}$ ratios.

Based on the results of these analyses, local strengthening interventions were recently carried out under the supervision of the

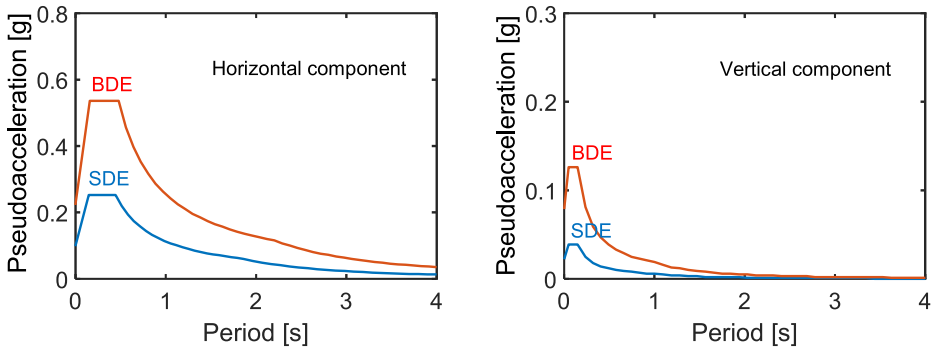

Fig. 18. Normative pseudo-acceleration elastic response spectra for Florence city — horizontal and vertical components.

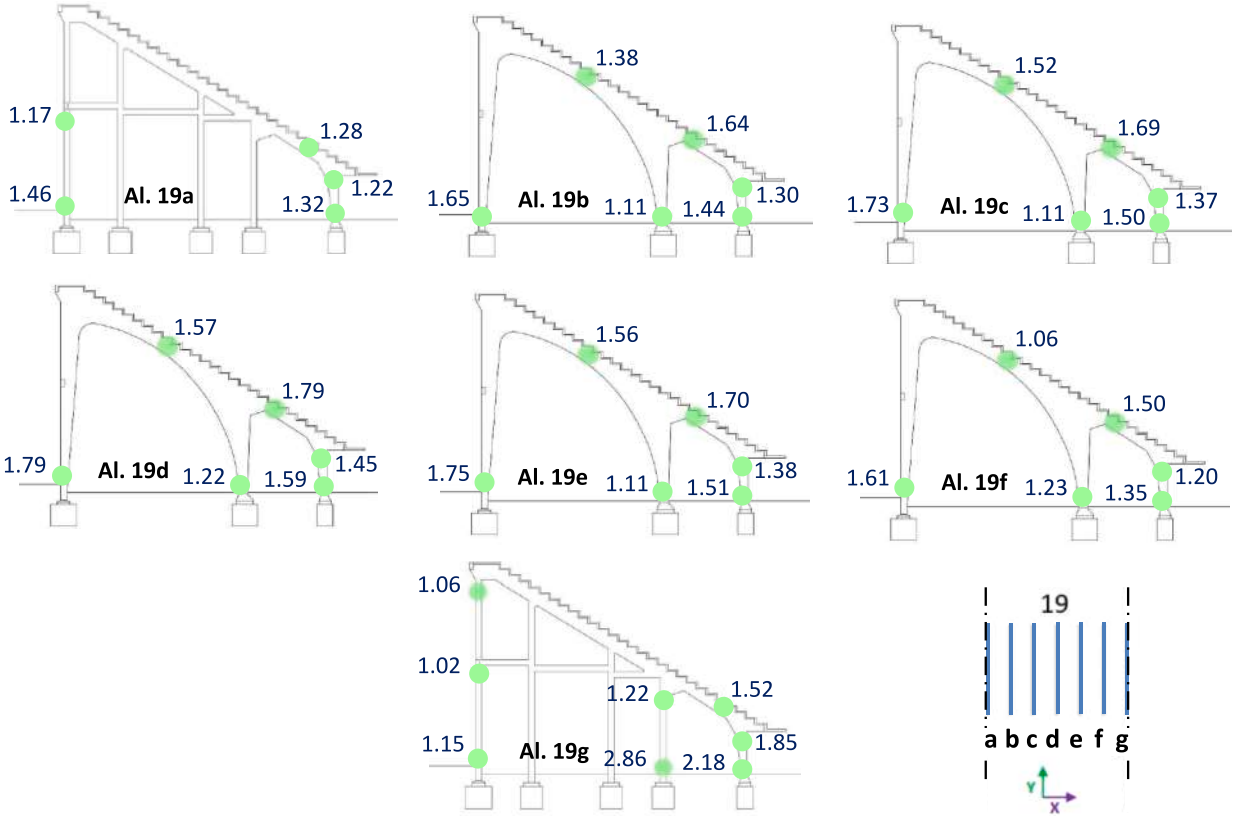

Fig. 19. Seismic analyses. Sections in unsafe conditions in compression-flexure (highlighted by green dots), and relevant demand/capacity ratios, for the frames belonging to block 19, with associated alignment numbering. (For interpretation of the references to colour in this figure legend, the reader is referred to the web version of this article.)

Technical Office of the Municipality of Florence, consisting in the application of carbon fiber reinforced polymer fabrics on the beams and columns in nominally unsafe conditions, in addition to extensive local repair measures based on reinforcing bar passivation and concrete cover repointing/reconstruction. Images of some of these interventions and the final repainting are displayed in Fig. 17.

The seismic assessment study in current conditions was carried out by modal superposition analyses, which were developed for the Serviceability Design Earthquake (SDE, with 63 % probability of being exceeded over the reference time period, V_R), and the Basic Design Earthquake (BDE, with 10 %/V_R probability) hazard levels assumed by the Italian Technical Standards. The V_R period is fixed at 75 years, obtained by multiplying the nominal structural life V_N of 50 years by a coefficient of use C_u equal to 1.5. This value is imposed to structures whose seismic resistance is of importance in view of the consequences associated with their possible collapse, including crowding-subjected sport facilities. By referring to topographic category T1 (flat surface), and C-type soil (deep deposits of dense or medium-dense sand, gravel or stiff clay from several ten to several hundred meters thick), the resulting peak ground accelerations for the two seismic levels referred to the city of Florence are as follows: 0.098 g (SDE), and 0.223 g (BDE), for the horizontal motion components; and 0.022 g (SDE), and 0.079 g (BDE), for the vertical component. Relevant elastic pseudo-acceleration response spectra at linear viscous damping ratio $\xi = 5$ % are plotted in Fig. 18. It is noted that site-specific seismic hazard data were not made available during the development of the study reported here. As a result, input actions were derived from Florence municipality-specific response spectra for the analyses both in current and retrofitted conditions.

The results of the analyses at the SDE highlight safe conditions for all members, whereas the BDE-related ones show 473 columns and 104 beams in unsafe conditions in compression-flexure, and 20 columns in shear (the latter being the shortest columns of Tribuna Centrale blocks 20, 21 and 22). The $\alpha_{D/C}$ ratios reach maximum values in compression-flexure equal to 2.86 for columns and 2.15 for beams, and 1.3 in shear. By way of example of these results, Fig. 19 summarizes the $\alpha_{D/C}$ ratios deriving from the seismic-related checks for the frames belonging to block 19, sketched in Fig. 16 above for static-related checks. The core structure of Maratona Tower and the underlying bearing frame structure and balcony, Tribuna Centrale cantilevered roof, and the three helical staircases are all in safe conditions. The same applies to the footings of all columns.

Based on the data drawn from these analyses, the seismic retrofit strategy adopted for the Stadium consists in the installation of dissipative braces incorporating pressurized fluid viscous (PFV) spring-dampers in several blocks, and PFV pure dampers across most separation gaps between adjacent blocks. By properly combining and jointly exploiting the damping capacities of the two types of PFV devices, this solution is aimed at minimizing the structural and architectural impact on the exposed RC structure, thanks to the inherently small visual perception both of the slender bracing system and the single dampers placed at the intrados of the crossed gaps.

6. Seismic retrofit design

The mechanical behaviour of the considered class of fluid viscous devices, whose working principle is based on the flow of a highly viscous fluid through a thin annular space between piston head and tank casing [28], is characterized by the following damping, F_d, and non-linear elastic, F_{ne}, force components [28–29]:

$$F_d(t) = csgn[\dot{x}(t)]|\dot{x}(t)|^{\gamma} \quad (1)$$

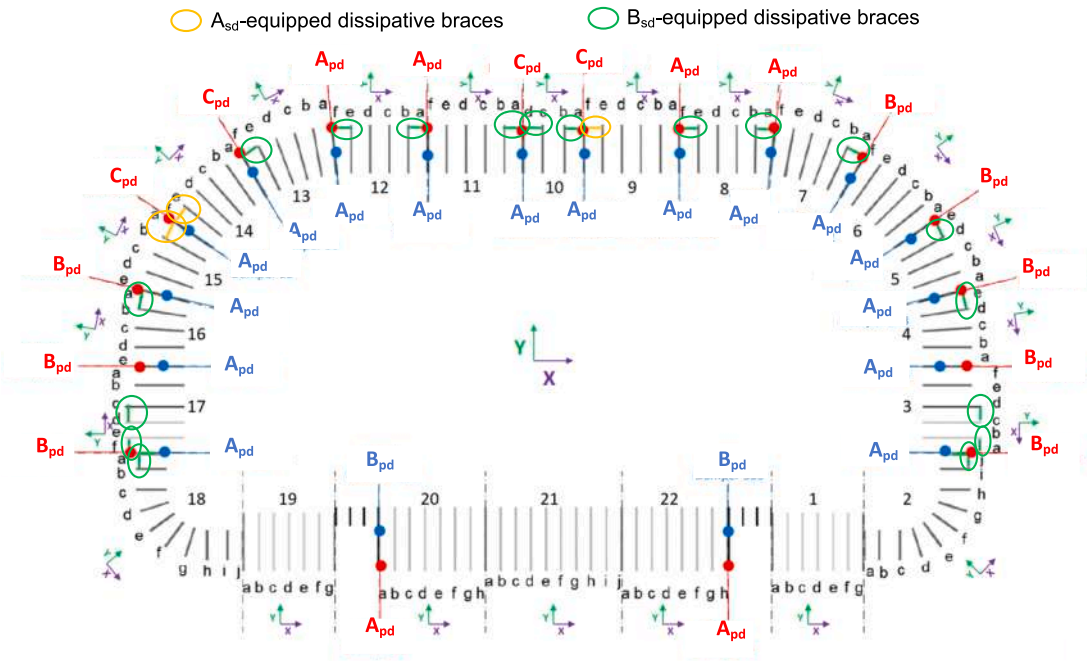

Fig. 20. Installation of the protection system in plan. Blue and red dots: PFV dampers mounted across separation gaps; green and yellow dashes highlighted by ellipses: dissipative braces incorporating PFV spring-dampers. (For interpretation of the references to colour in this figure legend, the reader is referred to the web version of this article.)

$$F_{ne}(t) = k_2 x(t) + \frac{(k_1 - k_2)x(t)}{\left[1 + \left|\frac{k_1 x(t)}{F_0}\right|^5\right]^{1/5}} \tag{2}$$

where: t = time variable; c = damping coefficient; $sgn(\cdot)$ = signum function; $\dot{x}(t)$= velocity; $|\cdot|$ absolute value: γ = fractional exponent, ranging from 0.1 to 0.2; F_0 = static pre-load; k_1, k_2 = stiffness of the response branches situated below and beyond F_0; and $x(t)$ = displacement. The two force components are co-existing in PFV spring-dampers, normally installed in dissipative bracing systems [30–31], where they are mounted in pairs, with pistons driven in half-stroke position at the tip of the supporting V-shaped steel trusses, so as to obtain a symmetric tension–compression response capacity. Pure dampers, characterized by the only dissipative component F_d, and originally manufactured to respond in tension–compression, are typically adopted to mitigate/prevent seismic pounding between adjacent buildings [25–26], or to act as classical dissipaters in internal bracing and exoskeleton systems [32–34].

The positions of dampers and dissipative braces selected in the retrofit design are highlighted in the plan of Fig. 20 by dots and dashes enclosed in ellipses, respectively. The dissipative braces are placed in longitudinal direction in all blocks belonging to Curva Fiesole, Maratona and Curva Ferrovia (except for block 6), plus one in transversal direction in blocks 2 and 18, for a total of 23 vertical alignments. Each longitudinal alignment is subdivided into three levels along the height, and thus incorporates three pairs of spring-dampers. The two transversal alignments include two levels only, due to the smaller height of the bleachers in blocks 2 and 18. Moreover, in these two alignments the spring-dampers are mounted only on the second level, since the displacements computed in current state are very small at the first level height. No dissipative braces are installed in the Tribuna Centrale blocks because they are heavily infilled, and thus very stiff to the horizontal translation. This hinders to adequately exploit the damping action of the PFV spring-dampers, in spite of their activation capacity also for small lateral displacements [35]. Based on these assumptions, the resulting total number of spring-dampers is equal to 130.

The pure dampers are mounted across the separation gaps of blocks 2 through 18, at an intermediate position (blue dots in Fig. 20) and on top (red dots) of the sloped beams of the constituting frames. Two dampers are installed also on the gaps between blocks 19 and 20, and blocks 1 and 22, respectively, since Tribuna Centrale lateral blocks 19 and 1 are infilled only up to half height in longitudinal direction, and thus they are prone to collision with the two stiffer adjacent blocks.

The protection system is sized by referring to the BDE hazard level, using the energy-based criterion proposed in [36], governed by the following relations:

$$E_{D,\alpha_{C/D}} = 2\pi\xi_{eq}\alpha_{C/D,max}V_{b,max}d_d \tag{3}$$

$$\xi_{eq} = \alpha_{C/D,max}V_{b,max}d_d\frac{2}{\pi}\frac{(\alpha_{C/D,max} - 1)}{\alpha_{C/D,max}} \tag{4}$$

where: $E_{D,}\alpha_{C/D}$ = energy dissipation tentatively assigned to the protective system, expressed as a function of the maximum demand/capacity ratio obtained from the assessment analysis in current state, $\alpha_{C/D,max}$; ξ_{eq} = equivalent viscous damping ratio; $V_{b,max}$ = maximum base shear calculated in current state; d_d = assumed design displacement. The criterion is separately applied to each block, by referring to the maximum stress state-related $\alpha_{C/D}$ value computed for its constituting members, and tentatively fixing d_d as maximum predictable top displacement in retrofitted conditions. A value of 50 mm is assumed for d_d, i.e. the hypothesized maximum width of the restored separation gaps after their planned cleaning, widening and waterproofing interventions. The gaps, currently 15-to-20 mm wide, are deteriorated by seepage and moister effects, which caused concrete cover cracking and loss, resulting in the formation of diffused little debris between the facing beams. The assumption of a d_d value coinciding with the hypothesized maximum width of the restored gaps is aimed at reaching no pounding effects in retrofitted conditions.

Based on these assumptions, the application of (3) and (4) leads to the following estimated value of the total energy dissipation demand: $E_{D,}\alpha_{C/D} = 3371$ kJ. Then, by referring to this value, the protective system is sized by separately considering the contributions offered by the dissipative braces and the gap-crossing dampers.

For the former, two types of spring-dampers in current production

Table 1
Mechanical characteristics of spring-dampers.

Device Type	E_n kJ	c kN(s/m)$^\gamma$	γ	F_{max} kN	s_{max} mm
A_{sd}	7	27.9	0.15	90	±30
C_{sd}	14	40	0.15	230	±40

Table 2
Mechanical characteristics of pure dampers.

Device Type	E_n kJ	c kN(s/m)$^\gamma$	γ	F_{max} kN	s_{max} mm
A_{pd}	9	176.2	0.1	±150	±30
B_{pd}	60	338.6	0.1	±300	±30
C_{pd}	80	451.2	0.1	±400	±50

[37] are selected, named A_{sd} and B_{sd}, by calibrating their choice on the displacement demand evaluated for the blocks in current conditions. The mechanical properties of the two types of devices, are as follows [37]: nominal energy dissipation capacity for the maximum response cycle, $E_n = 7$ kJ (A_{sd}), 14 kJ (B_{sd}); maximum response force, $F_{max} = 150$ kN (A_{sd}), 230 kN (B_{sd}); $c = 27.9$ kN·(s/m)$^\gamma$ (A_{sd}), 40 kN·(s/m)$^\gamma$ (B_{sd}); $\gamma =$ 0,15 (A_{sd} and B_{sd}), $F_0 = 90$ kN (A_{sd}), 130 kN (B_{sd}); stroke $s_{max} = \pm 30$ mm (A_{sd}), ± 40 mm (B_{sd}). These data are recapitulated in Table 1. The B_{sd} spring-dampers are installed in a bracing alignment of blocks 6, 10 and 14, for a total of three alignments and 18 devices; the remaining 112 ones are of A_{sd} type. The resulting total nominal energy dissipation capacity of the 130 spring-dampers corresponding to relevant maximum response cycles is: $E_{tnmc,sd} = (112{\cdot}7 + 18{\cdot}14)$ kJ = 1036 kJ. By considering that the energy dissipated in the smaller cycles produced by an earthquake scaled at the BDE intensity is approximately equal to 1.5 times $E_{tnmc,sd}$ [35–36], the total energy dissipation capacity of the spring-dampers, $E_{tn,sd}$, is evaluated as follows: $E_{tn,sd} = 1.5\ E_{tnmc,sd} = 1548$ kJ. Thus, the total nominal dissipation capacity to be tentatively assigned to the pure dampers, $E_{tn,pd,tent}$, is obtained as the difference between $E_{D,}\alpha_{C/D}$ and $E_{tn,sd}$: $E_{tn,pd,tent} = E_{D,}\alpha_{C/D} - E_{tn,sd} = (3371–1548)$ kJ = 1823 kJ.

Like for the spring-dampers incorporated in the dissipative braces, the choice of the pure dampers is based on the displacement demand on the blocks in current state. This leads to select three types of devices, named A_{pd}, B_{pd}, C_{pd}, with the following properties [37], listed in Table 2: $E_n = 9$ kJ (A_{pd}), 60 kJ (B_{pd}), 80 kJ (C_{pd}); $F_{max} = \pm 150$ kN (A_{pd}), ±300 kN (B_{pd}), ±400 kN (C_{pd}); $c = 176.2$ kN·(s/m)$^\gamma$ (A_{pd}), 338.6 kN·(s/m)$^\gamma$ (B_{pd}), 451.2 kN·(s/m)$^\gamma$ (C_{pd}); $\gamma = 0{,}1$ ($A_{pd,}$ B_{pd} and C_{pd}); $s_{max} = \pm 15$ mm (A_{pd}), ±50 mm (B_{pd}, C_{pd}). Dampers A_{pd} are placed at the intermediate levels of all sloped beams, except for the gaps between blocks 7 and 8, 8 and 9, 11 and 12, and 12 and 13, where they are installed also on top, and the gaps between blocks 19 and 20, and blocks 1 and 22, where they are positioned only on top. Dampers C_{pd} are located on top of gaps between blocks 9 and 10, 10 and 11, 13 and 14, and 14 and 15, and B_{pd} in the remaining positions. The not perfectly specular distribution in plan of B_{pd} and C_{pd} devices—in addition to the one adopted for the spring-dampers of the dissipative braces—is motivated by the fact that, although apparently symmetric with respect to the transversal axis in plan, the structure of the Stadium features some little asymmetries in the ring of stands. These are caused by the geometries of the staircases at the base of Maratona Tower and the three helical staircases, as well as by small differences in the cross sections of the sloped frames situated in opposite positions in plan. To recapitulate, 22 A_{pd}, 10 B_{pd} and 4 C_{pd} elements are adopted in total, which provides the following total nominal energy dissipation capacity of the 36 pure dampers for their maximum response cycles: $E_{tnmc,pd} = (22{\cdot}9 + 10{\cdot}60 + 4{\cdot}80)$ kJ = 1118 kJ. Like for the spring-dampers, a factor 1.5 is applied to estimate the total nominal dissipation capacity of the pure dampers, $E_{tn,pd}$, by accounting for the contribution of the smaller response cycles. This provides the following $E_{tn,pd}$ value: $E_{tn,pd} = 1.5\ E_{tnmc,pd} = 1677$ kJ, which is about 8 % lower than the tentatively estimated $E_{tn,pd,tent}$ value of 1823 kJ.

A complete view of the finite element model of the structure in retrofitted configuration is shown in Fig. 21. An overview of the response cycles of the most stressed spring-damper pair of each vertical alignment of the dissipative bracing system is presented in Figs. 22a-d, where the positions of the devices are highlighted with violet circles in the zoomed model views of the corresponding bleacher blocks. As visualized by these graphs, 9 out of the 21 most stressed spring-damper pairs in longitudinal direction are situated on the second level of the system, 9 on the first and 3 on the third, highlighting a balanced energy dissipation contribution of the devices for this installation layout. The maximum displacements range from 6.1 mm to 16.7 mm, for the A_{sd} elements, and from 7.7 mm to 14.7 mm, for the B_{sd} ones. These values slightly exceed 50 % (A_{sd}) and 35 % (B_{sd}) of the respective stroke capacities. The corresponding inter-level drifts of the bracing system normalized to relevant inter-level heights range from 0.16 % to 0.46 %.

Concerning the pure dampers, the response cycles of the two most stressed A_{pd}, B_{pd} and C_{pd} devices are plotted in Fig. 23. The maximum displacements are below the above-mentioned stroke limits (±30 mm—A_{pd}, ±50 mm—B_{pd} and C_{pd}). In addition to the two B_{pd} and two C_{pd} dissipaters referred to in Fig. 23, only the response of another B_{pd} device, connecting blocks 14 and 15, shows a maximum displacement exceeding 30 mm. This allows fixing the width of the restored gaps at the assumed d_d tentative design value of 50 mm only for the five gaps separating blocks 6 and 7, 10 and 11, 13 and 14, 14 and 15, and 17 and 18. For the remaining thirteen gaps across which the dampers are positioned, the post-restoration width could be limited to 30 mm.

The results in terms of stress states highlight reductions factors on the $\alpha_{D/C}$ ratios ranging from 1.09 to 1.83 for the 24 blocks, with a mean

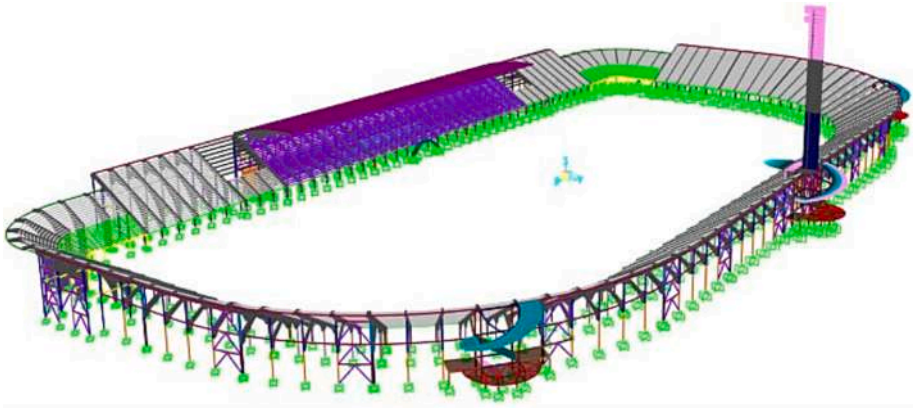

Fig. 21. View of the finite element model of the Stadium incorporating the dissipative bracing system and the pure dampers.

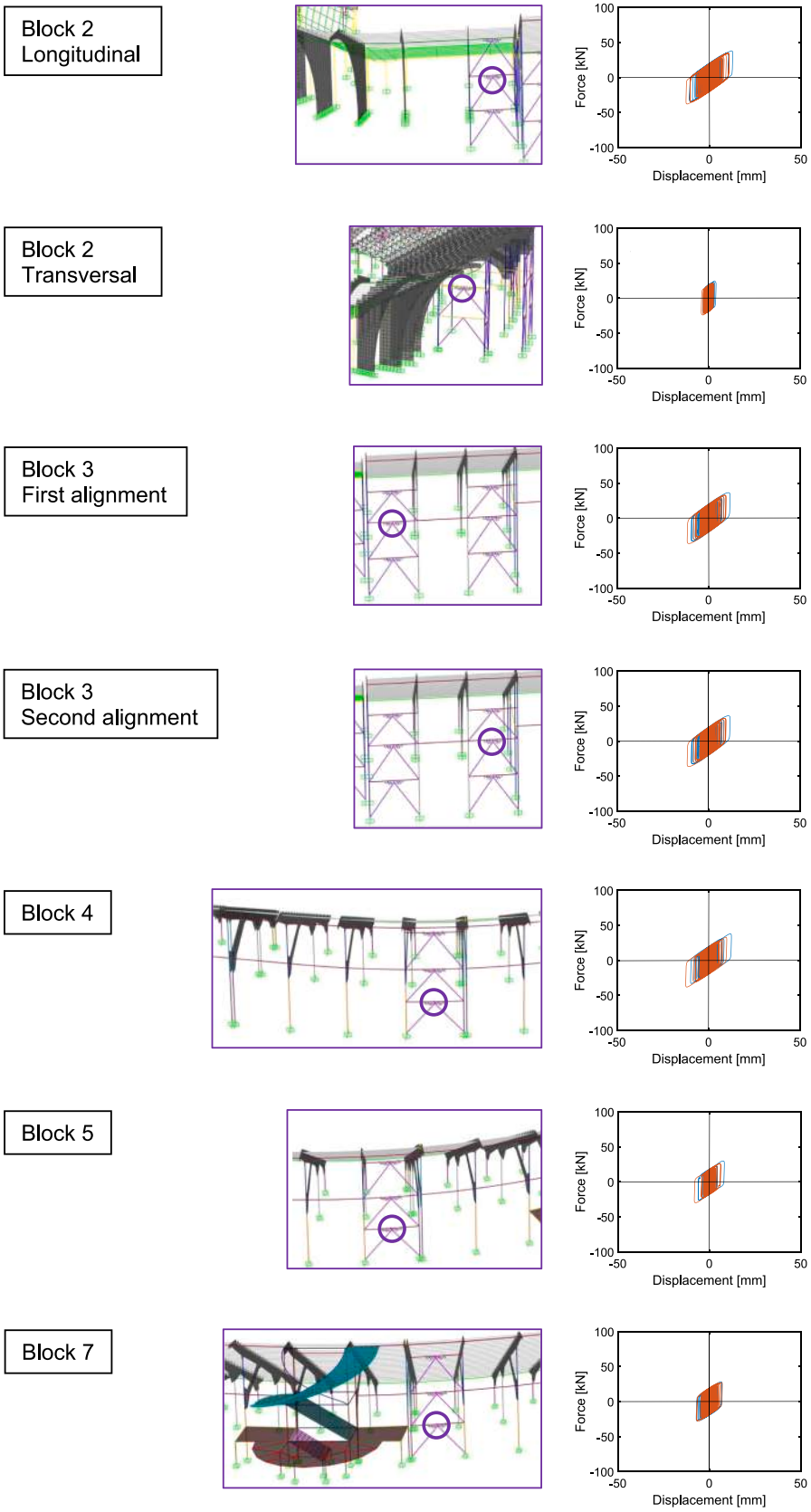

Fig. 22a. Positions, and response cycles at the BDE, of the most stressed spring-damper pairs (highlighted with violet circles) incorporated in the dissipative bracing system – blocks 2–7. (For interpretation of the references to colour in this figure legend, the reader is referred to the web version of this article.)

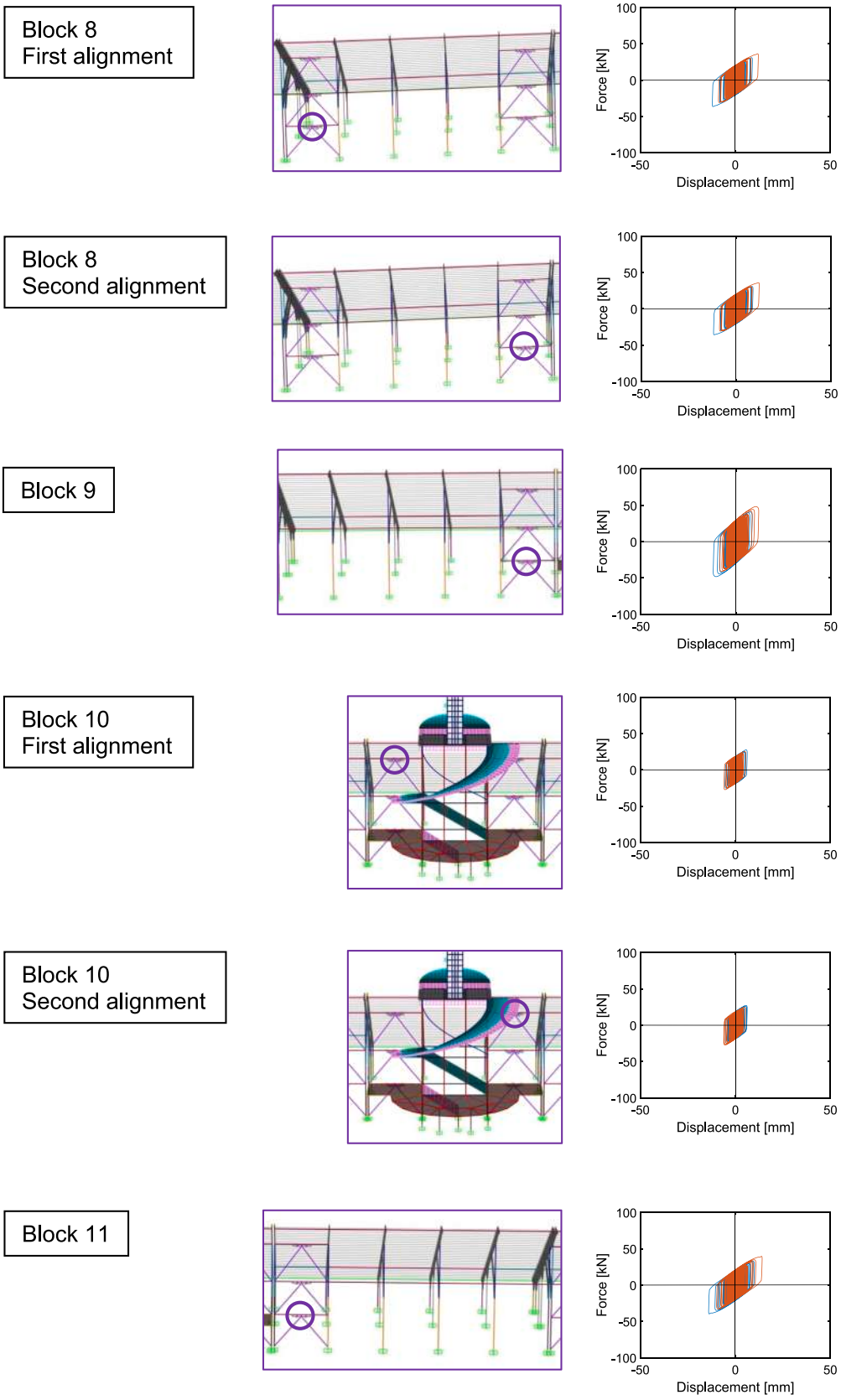

Fig. 22b. Positions, and response cycles at the BDE, of the most stressed spring-damper pairs (highlighted with violet circles) incorporated in the dissipative bracing system – blocks 8–11. (For interpretation of the references to colour in this figure legend, the reader is referred to the web version of this article.)

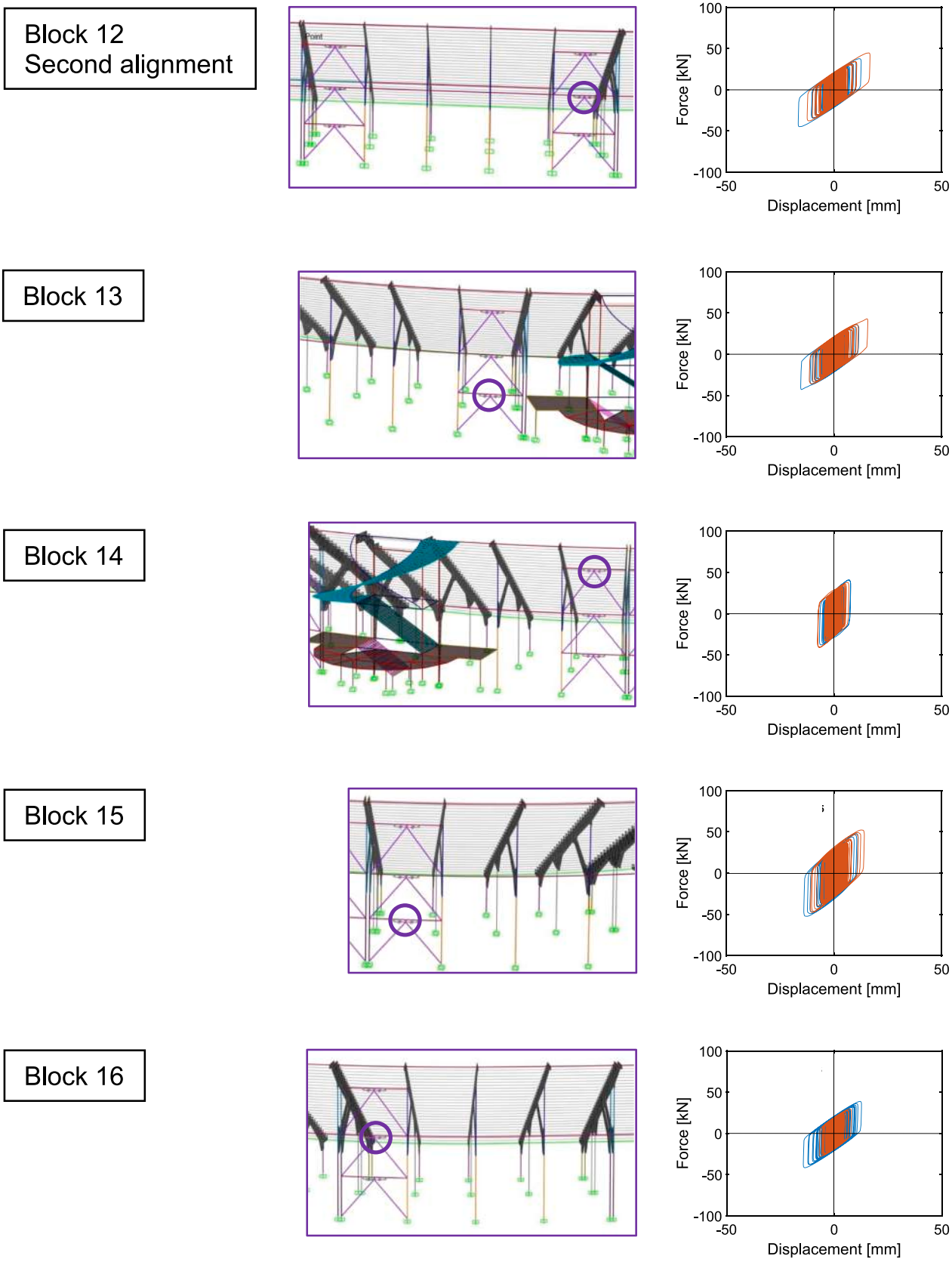

Fig. 22c. Positions, and response cycles at the BDE, of the most stressed spring-damper pairs (highlighted with violet circles) incorporated in the dissipative bracing system – blocks 12–16. (For interpretation of the references to colour in this figure legend, the reader is referred to the web version of this article.)

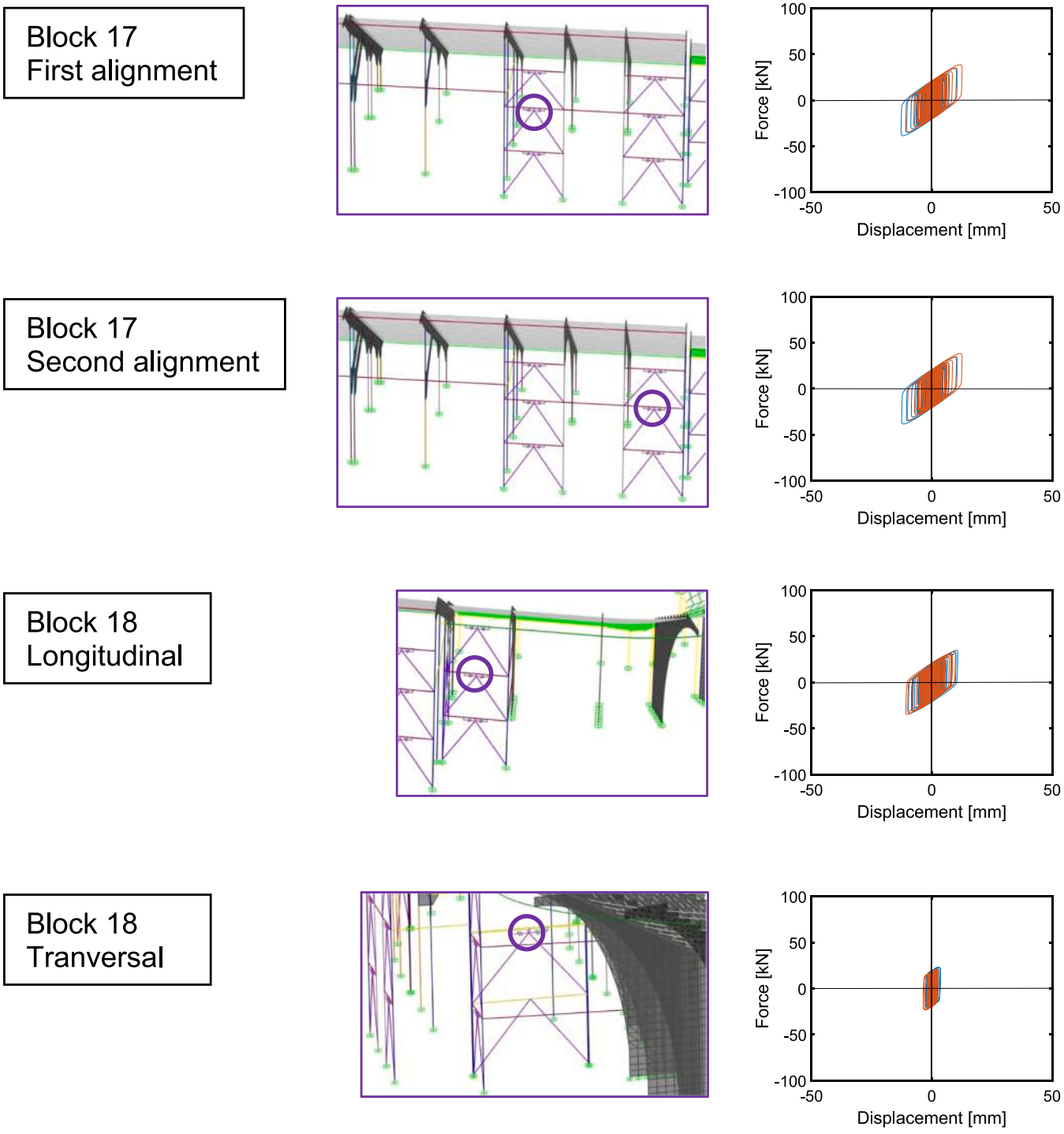

Fig. 22d. Positions, and response cycles at the BDE, of the most stressed spring-damper pairs (highlighted with violet circles) incorporated in the dissipative bracing system – blocks 17–18. (For interpretation of the references to colour in this figure legend, the reader is referred to the web version of this article.)

value of 1.31, as compared to current conditions. Thanks to these reductions, the sections in unsafe conditions in compression-flexure decrease to 209 (i.e. 44.4 % of sections in current state), for columns, and 41 (39.4 %), for beams, with maximum $\alpha_{D/C}$ ratios of 2.17 (columns) and 1.79 (beams). The shear checks are all met. By way of example of these results, the $\alpha_{D/C}$ ratios shown in Fig. 19 for block 19 in current state are duplicated, for retrofitted conditions, in Fig. 24.

Local strengthening interventions consisting in the application of one or two sheets of carbon fiber reinforced polymer fabrics, separately designed by professional technicians on behalf of the Municipality, in addition to the ones recently carried out to improve the response to static loads, allow achieving safe stress states in all beams and in 190 out of 209 columns. The remaining 19 columns, which should be wrapped with more than two fabrics sheets, can be alternatively strengthened by thin fiber reinforced grout-based jacketing interventions. No retrofit measure is required for all column footings also after the installation of the protection system.

The analyses were completed by examining different distributions of the spring-dampers and the pure dampers with respect to the basic design choice discussed here. In particular, the effects of the installation

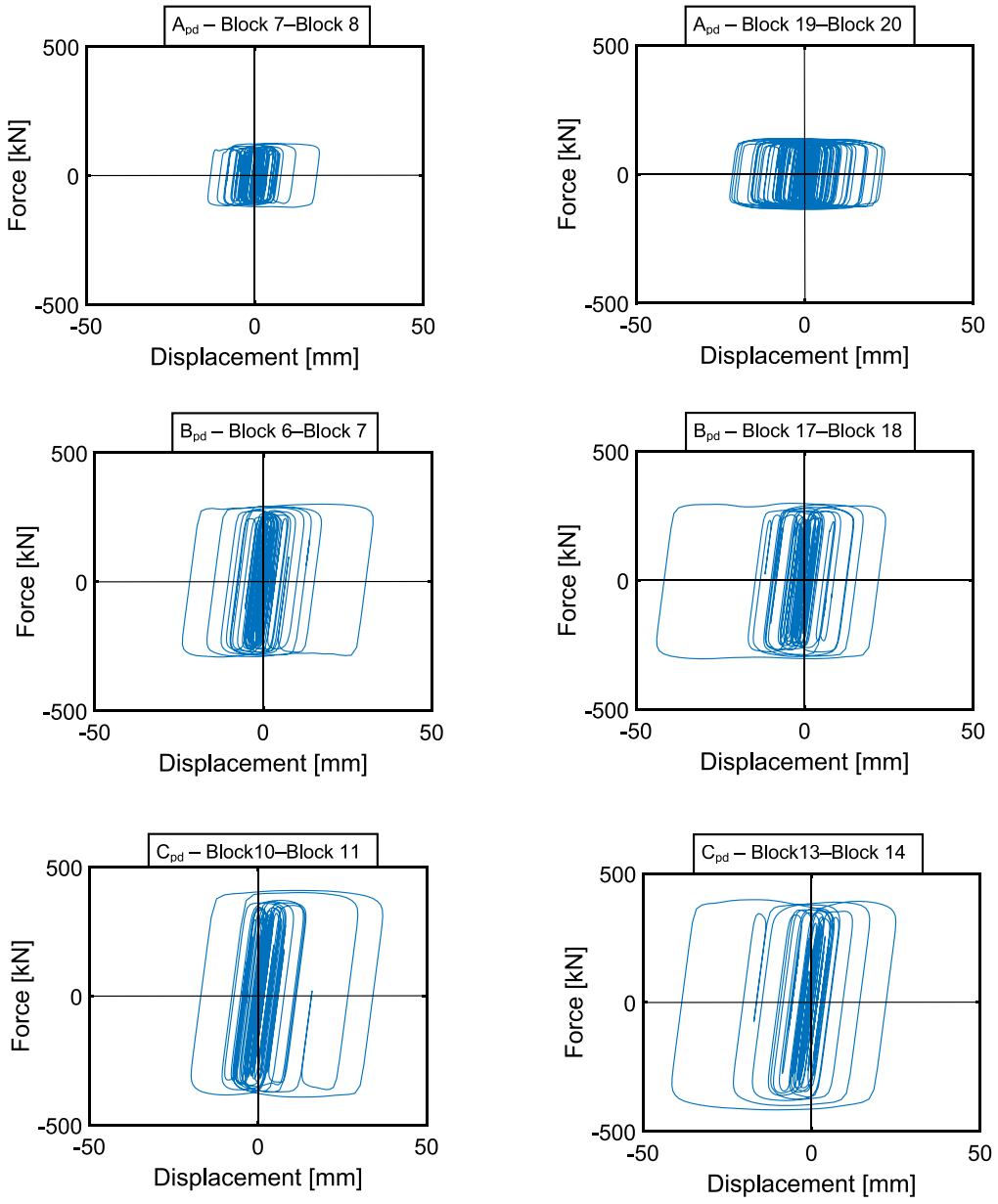

Fig. 23. Response cycles at the BDE of the most stressed A_{pd}, B_{pd} and C_{pd} pure dampers.

of B_{sd} spring-dampers in place of A_{sd} ones in various spans of the bracing system, and C_{pd} dampers in place of B_{pd} ones across some separation gaps, were investigated. As a general result of this enquiry, it was observed that the greater nominal energy dissipation capacities offered by these different options do not produce any growth in terms of actually dissipated energy (and thus, of seismic performance in retrofitted conditions), because of a delayed activation of several among the bigger spring-dampers and pure dampers, as compared to the designed layout. Therefore, the latter was confirmed as the final choice for the protective system, also in view of the lower cost associated to the smaller devices selected in it.

7. Conclusions

The diagnostic investigation campaign carried out on Artemio Franchi Stadium, in view of the restyling and modernization works recently planned on it, allowed initially evaluating acceptably good surface conservation conditions of the originally built RC structures, apart from physiological diffused degradation of concrete cover in the portions yet to be subjected to cover repair and finishing works currently under development. Furthermore, the technical separation gaps between the bleacher blocks appeared to be deteriorated by seepage and moister effects, with the formation of diffused little debris between the facing beams.

The information drawn from the original design documentation, as well as from the geometrical survey, testing campaigns on materials and structural members, and radar interferometric-based dynamic characterization tests carried out, helped gain the maximum normative knowledge level established by the Italian Technical Standards for existing buildings. This information was used to calibrate and progressively update the finite element model generated for the development of the performance assessment analyses in current conditions.

The latter offered the basis for the design of a static and seismic retrofit intervention on the Stadium, which had to be respectful of the preservation requirements imposed on its original RC structure by the Ministry for Cultural Heritage and Activities. This design was aimed at guaranteeing a safe use of the sports facility both in current conditions and after the upcoming restyling and modernization interventions,

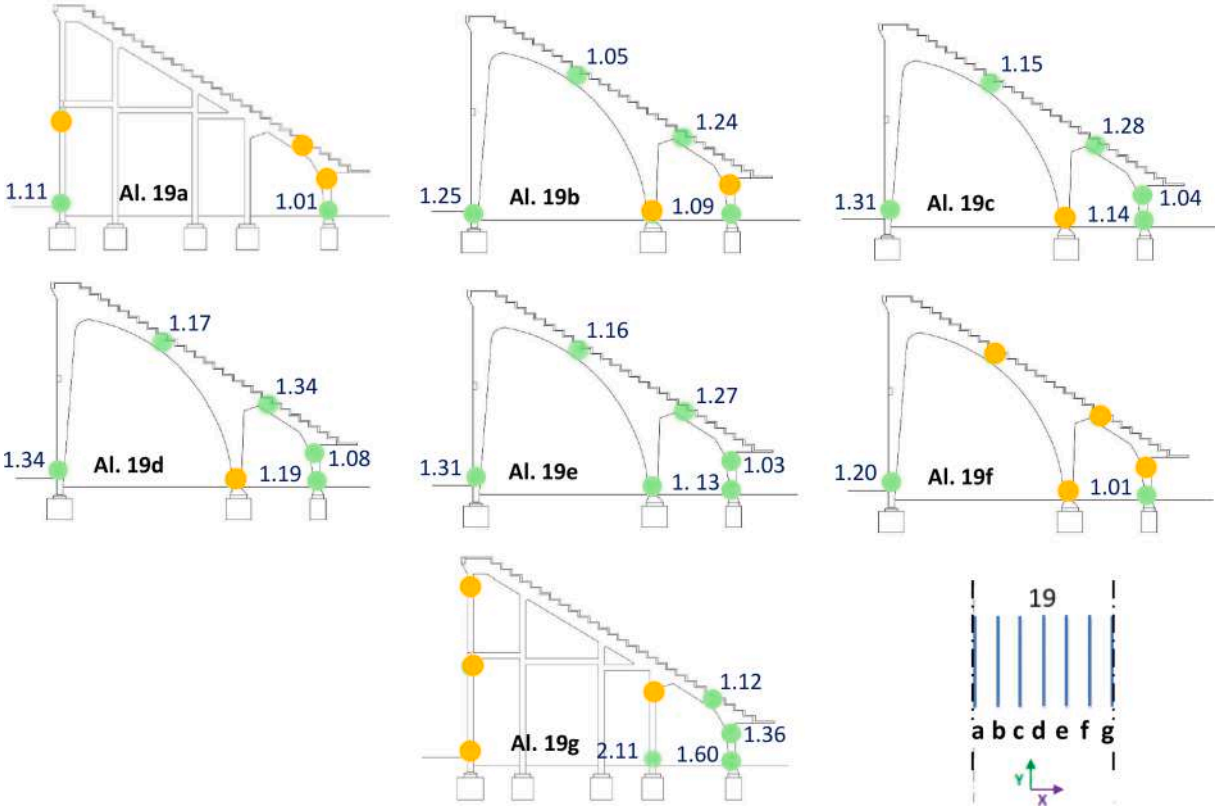

Fig. 24. Seismic analyses in retrofitted conditions. Sections in unsafe conditions in compression-flexure (highlighted by green dots), and relevant demand/capacity ratios, for the frames belonging to block 19, with associated alignment numbering. Orange dots denote sections passed to safe conditions.

whose structural additions are completely independent from the existing structures.

Specific remarks, arising from the performance and design study carried out, are summarized below.

- The compression strength of concrete evaluated by the laboratory tests on extracted samples and the on-site SonReb tests substantially confirmed the data specified in the acceptance test reports drafted at the end of the construction works. Similar f_{cm} values were found for Curva Ferrovia, Curva Fiesole and Tribuna Centrale blocks, equal to about 25 N/mm^2, and slightly higher for Maratona blocks. Notably higher f_{cm} values, equal to about 46 N/mm^2, were surveyed for the Maratona Tower RC core structure.
- The reinforcing steel yield stress experimentally identified for the extracted bars confirmed the results of the durometer tests carried out on the bars exposed by cover demolition, with values always greater than 300 N/mm^2.
- Nearly coinciding values of the three first vibration frequencies of Maratona Tower were deduced from the radar interferometric tests carried out under wind and spectators-induced dynamic excitations. Relevant results were also close to the values identified from the response of an accelerometer placed on the Tower roof terrace. The main vibration frequencies of the blocks were estimated by radar tests only on the basis of the spectators-induced response, due to their more massive structural characteristics.
- The finite element static analyses carried out at the ultimate limit state highlighted 87 sections in slightly unsafe conditions in flexure and compression-flexure, with average values of the demand/capacity ratios equal to 1.25 for columns and 1.18 for beams, and maximum values no greater than 1.5. At the same time, shear stress checks were always met. Based on these results, a first set of local strengthening interventions was recently developed, consisting in the application of carbon fiber reinforced polymer fabrics on the beams and columns in nominally unsafe static conditions.
- The seismic assessment analyses at the BDE showed 473 columns and 104 beams in unsafe conditions in compression-flexure, with maximum demand/capacity ratios equal to 2.86 for columns and 2.15 for beams, and 20 columns in shear, with peak ratios of 1.3.
- The data drawn from these checks prompted to design an advanced retrofit solution, consisting in the installation of 23 vertical alignments of dissipative steel braces incorporating PFV spring-dampers, for a total of 130 devices, and 36 PFV pure dampers across the technical separation gaps between adjacent blocks, except for those belonging to Tribuna Centrale, very stiff to the horizontal translation.
- This retrofit solution reduces the number of sections in unsafe conditions in compression-flexure to 44.4 % of the sections in current state, for columns, and 39.4 %, for beams, with maximum demand/capacity ratios scaled down to 2.17 (columns) and 1.79 (beams). Local strengthening interventions consisting in the application of carbon fiber reinforced polymer fabrics, in addition to the ones carried out to enhance the static response, determine safe stress states in all beams and 190 out of 209 columns. A jacketing intervention based on the use of fiber reinforced grout is suggested for the remaining 19 columns (the shortest ones of Tribuna Centrale blocks).
- The maximum displacements of 13 out of 18 pure dampers are below 30 mm. Therefore, the width of the restored gaps crossed by these dampers can be limited to this value. For the remaining gaps, the five dampers mounted on which reach peak displacements up to about 45 mm, the post-restoration width can coincide with the assumed tentative design value of 50 mm.
- The supplementary analyses carried out to check the effects of possible different distributions of the dissipaters, with respect to the basic design solution, showed that replacing A_{sd} spring-dampers with B_{sd} ones in some spans of the bracing system, and B_{pd} with C_{pd}

dampers on some gaps does not increase the dissipated energy, as a consequence of a delayed activation of the bigger devices. This corroborates the device choices resulting from the preliminary sizing process.

CRediT authorship contribution statement

Gloria Terenzi: Conceptualization, Methodology, Investigation, Data curation, Validation, Visualization, Supervision, Writing – review & editing, Funding acquisition. **Elena Fuso:** Software, Investigation, Data curation, Validation, Visualization. **Stefano Sorace:** Methodology, Validation, Writing – review & editing.

Declaration of Competing Interest

The authors declare that they have no known competing financial interests or personal relationships that could have appeared to influence the work reported in this paper.

Data availability

The authors do not have permission to share data.

Acknowledgements

The study reported in this paper was sponsored by the Municipality of Florence under Grant nr. DD/2021/05652 and by the Italian Department of Civil Protection within the ReLUIS-DPC Project 2022/2024, WP 15 “Normative Contributions on Seismic Isolation and Dissipation”. The authors gratefully acknowledge this financial support.

References

[1] Billington DP. The tower and the bridge: the new art of structural engineering. New York (NY): Basic Books; 1983.
[2] Hu N, Feng P, Dai GL. Structural art: Past, present and future. Eng Struct 2014;79:407–16.
[3] Nervi PL. Scienza o arte del costruire? Rome (Italy): Edizioni della Bussola; 1945 [in Italian].
[4] Nervi PL. Aesthetics and technology in building. Cambridge (USA): Harvard University Press; 1965.
[5] Dorfles G. L’architettura moderna. 6th Ed. Milan (Italy): Garzanti; 1975 [in Italian].
[6] Frampton K. Modern architecture: A critical history. London (UK), New York (NY): Thames & Hudson; 2007.
[7] Michelucci G. Lo stadio “Giovanni Berta” in Firenze dell’ingegnere Pier Luigi Nervi. Architettura 1932; XI:105–116 [in Italian].
[8] Abraham G. Le stade Giovanni Berta à Florence. Ingénieur: Pier Luigi Nervi. Le Technique des Travaux 1933; IX:93-101 [in French].
[9] Pagano G. Ing. Pier Luigi Nervi, Stadio Berta a Firenze. Casabella 1933; IV:38–41 [in Italian].
[10] Bardi PM. Lo Stadio di Firenze Casabella 1933;64:4–11 [in Italian].
[11] Nervi PL. Considerazioni tecniche e costruttive sulle gradinate e pensiline per stadi. Casabella 1933;64:10–1.
[12] Pagano G. Stades à l’étranger: Stade G. Berta, Ingégnieur architect: Pier Luigi Nervi. L’Architecture d’aujourd’hui 1934; 3:31–35 [in French].
[13] Legislative Decree 22 January 2004, n. 42 Code of cultural and landscape heritage, pursuant to article 10 of the law of 6 July 2002, no. 137. Rome (Italy): Italian Ministry of Cultural Heritage and Activities, GU nr. 45; 24 February 2004 [in Italian].
[14] Sorace S, Terenzi G. Structural assessment of a modern heritage building. Eng Struct 2013;49:743–55.
[15] Foti D. Shear vulnerability of old historical existing R.C. structures. Int J Arch Heritage: Conserv, Analy, Restoration 2015;9(4):453–67.
[16] Sorace S, Terenzi G. Analysis and seismic isolation of an older reinforced concrete vaulted building. Contemporary Eng Sci 2016;9:1201–15.
[17] Terenzi G, Fuso E, Sorace S, Costoli I. Enhanced seismic retrofit of a reinforced concrete building of architectural interest. Buildings 2020;10:211_1 -17.
[18] Diaferio M, Foti D, Lerna M, Sabbà F. A procedure for the seismic risk assessment of the cultural heritage. Bull Earthq Eng 2021;19:1027–50.
[19] Ministerial Decree 17 January 2018. Update of Technical Standards for Constructions. Rome (Italy): Italian Ministry of Infrastructure and Transport, GU no. 42 [in Italian].
[20] Circular 21 January 2019 no. 7. Instructions for the application of the Update of Technical Standards for Constructions. Rome (Italy): Ministry of Infrastructure and Transport, Ordinary supplement to G.U. no. 35 [in Italian].
[21] Pieraccini M, Miccinesi L, Terenzi G, Costoli I, Spinelli P, Mazzieri G. Structural health monitoring of “Artemio Franchi” Stadium in Florence, Italy: Measurement using interferometric radar. In: Proceedings of the 5th Int. Conference on Smart Monitoring, Assessment and Rehabilitation of Civil Structures, SMAR 2019. Potsdam, Germany; 2019, paper we.2.d.8, 8 pp.
[22] CSI. SAP2000NL. Theoretical and user’s manual. Release 24.06. Computers & Structures Inc., Berkeley, CA, USA, 2023.
[23] Mazza F, Donnici A. In-plane and out-of-plane seismic damage of masonry infills in existing r.c. structures: the case study of De Gasperi-Battaglia school in Norcia. Bull Earthq Eng 2021;19(1):345–76.
[24] Sorace S, Costoli I, Terenzi G. Seismic assessment and dissipative bracing retrofit-based protection of infills and partitions in RC structures. Eng Struct 2023;2023 (281):115781.
[25] Pratesi F, Sorace S, Terenzi G. Analysis and mitigation of seismic pounding of a slender R/C bell tower. Eng Struct 2014;71:23–34.
[26] Licari M, Sorace S, Terenzi G. Nonlinear modeling and mitigation of seismic pounding between R/C frame buildings. J Earthq Eng 2015;19:431–60.
[27] Royal Decree 13 March 1927. New Technical and Hygienic Standards for Seismic Constructions. Rome (Italy): GU nr. 82 [in Italian].
[28] Sorace S, Terenzi G. Non-linear dynamic modelling and design procedure of FV spring-dampers for base isolation. Eng Struct 2001;23:1556–67.
[29] Pekcan G, Mander JB, Chen SS. The seismic response of a 1: 3 scale model R.C. structure with elastomeric spring dampers. Earthq Spectra 1995;11:249–67.
[30] Sorace S, Terenzi G, Fadi F. Shaking table and numerical seismic performance evaluation of a fluid viscous-dissipative bracing system. Earthq Spectra 2012;28:1619–42.
[31] Sorace S, Terenzi G, Bertino G. Viscous dissipative, ductility-based and elastic bracing design solutions for an indoor sports steel building. Adv Steel Constr 2012;8:295–316.
[32] Foti D. Response of frames seismically protected with passive systems in near-field areas. Int J Struct Eng 2014;5:326–45.
[33] Mazza F. Combination of different types of damped braces for two-level seismic control of rc framed buildings. Journal of Building. Engineering 2021;44. art. no. 103268.
[34] Mazza F. Dissipative steel exoskeletons for the seismic control of reinforced concrete framed buildings. Struct Control Health Monit 2021;28. art. no. e2683.
[35] Terenzi G, Costoli I, Sorace S. Activation control extension of a design method of fluid viscous dissipative bracing systems. Bull Earthq Eng 2020;18(8):4017–38.
[36] Terenzi G. Energy-based design criterion of dissipative bracing systems for seismic retrofit of framed structures. Appl Sci 2018;8(2):268.
[37] Dyna Shock System. URL http://www.dynashocksystem.com/ [accessed 13 May 2023].